Characteristics of Kepler Planetary Candidates Based on the First Data Set

The Astrophysical Journal, 728:117 (20pp), 2011 February 20 doi:10.1088/0004-637X/728/2/117

CHARACTERISTICS OF *KEPLER* PLANETARY CANDIDATES BASED ON THE FIRST DATA SET

William J. Borucki[1], David G. Koch[1], Gibor Basri[2], Natalie Batalha[3], Alan Boss[4], Timothy M. Brown[5], Douglas Caldwell[6], Jørgen Christensen-Dalsgaard[7], William D. Cochran[8], Edna DeVore[6], Edward W. Dunham[9], Andrea K. Dupree[10], Thomas N. Gautier III[11], John C. Geary[10], Ronald Gilliland[12], Alan Gould[13], Steve B. Howell[14], Jon M. Jenkins[6], Hans Kjeldsen[7], David W. Latham[10], Jack J. Lissauer[1], Geoffrey W. Marcy[2], David G. Monet[15], Dimitar Sasselov[10], Jill Tarter[6], David Charbonneau[10], Laurance Doyle[6], Eric B. Ford[16], Jonathan Fortney[17], Matthew J. Holman[10], Sara Seager[18], Jason H. Steffen[19], William F. Welsh[20], Christopher Allen[21], Stephen T. Bryson[1], Lars Buchhave[10], Hema Chandrasekaran[6], Jessie L. Christiansen[6], David Ciardi[22], Bruce D. Clarke[6], Jessie L. Dotson[1], Michael Endl[8], Debra Fischer[23], Francois Fressin[10], Michael Haas[1], Elliott Horch[24], Andrew Howard[2], Howard Isaacson[2], Jeffery Kolodziejczak[25], Jie Li[6], Phillip MacQueen[8], Søren Meibom[10], Andrej Prsa[26], Elisa V. Quintana[6], Jason Rowe[1], William Sherry[14], Peter Tenenbaum[6], Guillermo Torres[10], Joseph D. Twicken[6], Jeffrey Van Cleve[6], Lucianne Walkowicz[2], and Hayley Wu[6]

[1] NASA Ames Research Center, Moffett Field, CA 94035, USA; William.J.Borucki@nasa.gov
[2] University of California, Berkeley, CA 94720, USA
[3] San Jose State University, San Jose, CA 95192, USA
[4] Carnegie Institute of Washington, Washington, DC 20015, USA
[5] Las Cumbres Observatory Global Telescope, Goleta, CA 93117, USA
[6] SETI Institute, Mountain View, CA 94043, USA
[7] Aarhus University, Aarhus, Denmark
[8] McDonald Observatory, University of Texas at Austin, Austin, TX 78712, USA
[9] Lowell Observatory, Flagstaff, AZ 86001, USA
[10] Harvard-Smithsonian Center for Astrophysics, Cambridge, MA 02138, USA
[11] Jet Propulsion Laboratory, California Institute of Technology, Pasadena, CA 91109, USA
[12] Space Telescope Science Institute, Baltimore, MD 21218, USA
[13] Lawrence Hall of Science, Berkeley, CA 94720, USA
[14] NOAO, Tucson, AZ 85719, USA
[15] United States Naval Observatory, Flagstaff, AZ 86001, USA
[16] University of Florida, Gainesville, FL 32611, USA
[17] University of California, Santa Cruz, CA 95064, USA
[18] MIT, Cambridge, MA 02139, USA
[19] Fermilab, Batavia, IL 60510, USA
[20] San Diego State University, San Diego, CA 92182, USA
[21] Orbital Sciences Corp., Mountain View, CA 94043, USA
[22] Exoplanet Science Institute/Caltech, Pasadena, CA 91125, USA
[23] Yale University, New Haven, CT 06520, USA
[24] Southern Connecticut State University, New Haven, CT 06515, USA
[25] MSFC, Huntsville, AL 35805, USA
[26] Villanova University, Villanova, PA 19085, USA
Received 2010 July 21; accepted 2010 December 13; published 2011 January 28

ABSTRACT

In the spring of 2009, the *Kepler* Mission commenced high-precision photometry on nearly 156,000 stars to determine the frequency and characteristics of small exoplanets, conduct a guest observer program, and obtain asteroseismic data on a wide variety of stars. On 2010 June 15, the *Kepler* Mission released most of the data from the first quarter of observations. At the time of this data release, 705 stars from this first data set have exoplanet candidates with sizes from as small as that of Earth to larger than that of Jupiter. Here we give the identity and characteristics of 305 released stars with planetary candidates. Data for the remaining 400 stars with planetary candidates will be released in 2011 February. More than half the candidates on the released list have radii less than half that of Jupiter. Five candidates are present in and near the habitable zone; two near super-Earth size, and three bracketing the size of Jupiter. The released stars also include five possible multi-planet systems. One of these has two Neptune-size (2.3 and 2.5 Earth radius) candidates with near-resonant periods.

Key words: planets and satellites: detection – surveys

Online-only material: color figures

1. INTRODUCTION

Kepler is a Discovery-class mission designed to determine the frequency of Earth-size planets in and near the habitable zone (HZ) of solar-type stars. The instrument consists of a 0.95 m aperture telescope/photometer designed to obtain high-precision photometric measurements of >100,000 stars to search for patterns of transits. The focal plane of the Schmidt-type telescope contains 42 CCDs with a total of 95 megapixels that cover 115 deg^2 of sky. *Kepler* was launched into an Earth-trailing heliocentric orbit on 2009 March 6, finished its commissioning on 2009 May 12, and is now in science operations mode. Further details of the *Kepler* Mission and instrument can be found in Koch et al. (2010b), Jenkins et al. (2010c), and Caldwell et al. (2010).

During the commissioning period, photometric measurements were obtained at a 30-minute cadence for 53,000 stars for 9.7 days. During the first 33.5 days of science-mode operation, 156,097 stars were similarly observed. Five new exoplanets with sizes between 0.37 and 1.6 Jupiter radii and orbital periods from 3.2 to 4.9 days were confirmed by radial velocity (RV) observations (Borucki et al. 2010; Koch et al. 2010a; Dunham et al. 2010; Jenkins et al. 2010a; Latham et al. 2010).

The results discussed in this paper are based on the first data segment taken at the beginning of science operations on 2009 May 13 UT and finished on 2009 15 June 15 UT; a 33.5-day segment (labeled Q1).

The observations used *Kepler*'s normal list of 156,097 exoplanet target stars. The *Kepler* K_p bandpass covers both the V and R photometric passbands. These stars are primarily main-sequence dwarfs chosen from the *Kepler* Input Catalog (KIC). Stars were chosen to maximize the number of stars that were both bright and small enough to show detectable transit signals for small planets in and near the HZ (Batalha et al. 2010). Most stars were in the magnitude range $9 < K_p < 16$.

Data for all stars are recorded at a cadence of one per 29.4 minutes (hereafter, long cadence, or LC). Data for a subset of 512 stars are also recorded at a cadence of one per 58.5 s (hereafter, short cadence or SC), sufficient to conduct asteroseismic observations needed for measurements of the stars' size, mass, and age. The results presented here are based only on LC data. For a full discussion of the LC data and their reduction, see Jenkins et al. (2010b, 2010c); see Gilliland et al. (2010) for a discussion of the SC data.

At the one-year anniversary of the receipt of the first set of data from the beginning of science operations, the data for 156,097 stars covering these two periods are now available to the public, apart from two exceptions: 400 stars held back to allow completion of one season of observations by the *Kepler* team, and 2778 stars held back for the Guest Observers and Asteroseismic Science Consortium (KASC). These data will be released on 2011 February 1, and in 2010 November when the proprietary period is complete, respectively. A total of 152,919 stars are now available at several levels of processing at the Multi-Mission Archive at the Space Telescope Science Institute (MAST[27]) for analysis by the community.

2. DESCRIPTION OF THE DATA

Because of great improvements to the data-processing pipeline, many more candidates are readily visible than in the data used for the papers published in early 2010. During the early phase of operations, many of the candidates were found by visual inspection, but with recent improvements to the analysis pipeline, most are now being detected in an automated fashion. Over 855 stars with transiting exoplanet signatures have been identified. Of those, approximately 150 have been identified as likely false positives and, consequently, removed from consideration as viable exoplanet candidates.

A separate paper that identifies false positive events found in the released data will be submitted. In the interim, see the list at the MAST. False positive events are patterns of dimming that appear to be the result of planetary transits, but are actually caused by other astrophysical processes or by instrumental fluctuations in the brightness values that mimic planetary transits. The identification of the false positives should help the community avoid wasting observation resources.

Data and search techniques capable of finding planetary transits are also very sensitive to eclipsing binary (EB) stars, and indeed the number of EBs discovered with *Kepler* vastly exceeds the number of planetary candidates. With more study, some of the current planetary candidates might also be shown to be EBs. Prsa et al. (2010) present a list of EBs with their basic system parameters that have been detected in these early data.

The discussion in this paper covers the 305 stars with candidates that the *Kepler* team does not plan to give high priority for follow-up confirmation. These are generally faint stars and were not observed for the first 9.7-day time interval. Thus, only 33.5 days of data are available for most candidates discussed herein. An Appendix identifying these candidates and providing their characteristics is attached.

2.1. Selecting the Candidates to Release

The candidates discussed here do not include 400 stars selected as high-priority targets. These are primarily those amenable to ground-based follow-up observations and those with the smallest candidates. In particular, these stars include (1) those showing two or more sets of transit events at distinctly different periods, (2) those showing any indication of transit-timing variations that could lead to detection of additional planets, (3) stars cooler than 4000 K, (4) stars brighter than $K_p = 13.9$, (5) candidates with a likelihood of showing a secondary occultation event, and (6) stars with candidates smaller than 1.5 $R_\oplus$. The likelihood of an occultation event is determined by computing the ratio of the stellar luminosity to the thermal emission of the planet assuming an even distribution of energy over the day and night side of the planet, an albedo of 0.1, and a circular orbit at a distance given by the stellar properties in the KIC and the period provided by the transit photometry. This ratio is then compared to the expected photometric noise given the apparent brightness of the star in question. Targets are flagged if the occultation depth is expected to be larger than 2σ. Collectively, these criteria yielded 400 stars, though the large majority of candidates were selected simply based on the brightness cutoff (e.g., amenability to ground-based follow-up observations). These targets will be released to the public in 2011 February, giving the team a full observing season to collect follow-up observations that will help to weed out astrophysical false positives. The remaining 305 stars comprise the sample described herein.

2.2. Noise Sources in the Data

The *Kepler* photometric data contain a wide variety of both random and systematic noise sources. Random noise sources such as shot noise from the photon flux and read noise have (white) Gaussian distributions. Stellar variability introduces red (correlated) noise. For many stars, stellar variability is the largest noise source. There are also many types of instrument-induced noise: pattern noise from the clock drivers for the "fine-guidance" sensors, start-of-line ringing, overshoot/undershoot due to the finite bandwidth of the detector amplifiers, and signals that move through the output produced by some of the amplifiers that oscillate. The latter noise patterns (which are typically smaller than one least-significant-bit in the digital-to-analog converter for a single read operation) are greatly affected by slight temperature changes, making their removal difficult. Noise due to pointing drift, focus changes, differential velocity aberration, CCD defects, cosmic ray events, reaction wheel heater cycles, breaks in the flux time series due to desaturation of the reaction wheels, spacecraft upsets, monthly rolls to downlink the data, and quarterly rolls to re-orient the spacecraft to keep the solar panels pointed at the Sun are also present.

[27] http://archive.stsci.edu/kepler/kepler_fov/search.php

These sources and others are treated in Jenkins et al. (2010b) and Caldwell et al. (2010). Work is underway to improve the mitigation and flagging of the affected data. Additional noise sources are seen in the short cadence data (Gilliland et al. 2010). In particular, a frequency analysis of these data often shows spurious regularly spaced peaks at 48.9388 day^{-1} and their harmonics. Additionally, there appears to be a noise source that causes additive offsets in the time domain inversely proportional to stellar brightness.

Because of the complexity of the various small effects that are important to the quality of the *Kepler* data, prospective users of *Kepler* data are strongly urged to study the data release notes (hosted at the MAST) for the data sets they intend to use. Note that the *Kepler* data analysis pipeline was designed to perform differential photometry to detect planetary transits so other uses of the data products require caution.

2.3. Distinguishing Planetary Candidates from False Positive Events

Stars that show a pattern consistent with those from a planet transiting its host star are labeled "planetary candidates." Those that were at one time considered to be planetary candidates, but subsequently failed some consistency test, are labeled "false positives." Thus, the search for planets starts with a search of the time series of each star for a pattern that exceeds a detection threshold commensurate with a non-random event. After passing all consistency tests described below, and only after a review of all the evidence by the entire *Kepler* Science Team, does the candidate become a validated exoplanet. It is then submitted to a peer-reviewed journal for publication.

There are two general types of processes associated with false positive events in the *Kepler* data that must be evaluated and eliminated before a candidate planet can be considered a valid discovery: (1) statistical fluctuations or systematic variations in the time series, and (2) astrophysical phenomena that produce similar signals. A sufficiently high threshold has been used that statistical fluctuations should not contribute to the candidates proposed here. Similarly, systematic variations in the data have been interpreted in a conservative manner and only rarely should result in false positives. However, astrophysical phenomena that produce transit-like signals will be much more common.

2.4. Search for False Positives in the Output of the Data Pipeline

The Transiting Planet Search (TPS) pipeline searches through each systematic error-corrected flux time series for periodic sequences of negative pulses corresponding to transit signatures. The approach is a wavelet-based, adaptive matched filter that characterizes the power spectral density (PSD) of the background process yielding the observed light curve and uses this time-variable PSD estimate to realize a pre-whitening filter and whiten the light curve (Jenkins 2002; Jenkins et al. 2010c, 2010d). Transiting Planet Search then convolves a transit waveform, whitened by the same pre-whitening filter as the data, with the whitened data to obtain a time series of single event statistics. These represent the likelihood that a transit of that duration is present at each time step. The single event statistics are combined into multiple event statistics by folding them at trial orbital periods ranging from 0.5 days to as long as one quarter (∼90 days). The step sizes in period and epoch are chosen to control the minimum correlation coefficient between neighboring transit models used in the search so as to maintain a high sensitivity to transit sequences in the data. The transit durations used for TPS through 2010 June were 3, 6, and 12 hr. These transit durations will be augmented to include 1.5, 2.0, 2.5, 3.0, 4.0, 5.0, 6.0, 7.5, 9.5, 12.0, and 15.0 hr in order to maintain a similar degree of sensitivity as that achieved for epoch and period. This modification should increase the sensitivity to low signal-to-noise ratio (S/N) signals. Transiting Planet Search is also being modified to conduct searches across the entire mission duration by "stitching" quarterly segments together so that we can identify periods longer than one quarter in the data.

The maximum multiple event statistics is collected for each star and those with maximum multiple event statistics greater than 7.1σ are flagged as threshold crossing events (TCEs). The Data Validation (DV) pipeline fits limb-darkened transit models to each TCE and performs a suite of diagnostic tests to build or break confidence in each TCE as a planetary signature as opposed to an EB or noise fluctuation (Wu et al. 2010; Tenenbaum et al. 2010). Data Validation removes the transit signature from the light curve and searches for additional transiting planets using a call to TPS. Threshold crossing events with transit depths more than 15% are not processed by DV since they are most likely to be EBs. Also, currently light curves whose maximum multiple event statistics are less than 1.25 times the maximum single event statistic are not processed by DV since these are likely due to one large single event, and most of these cases are due to radiation-induced step discontinuities introduced at the pixel level.

Using these estimates and information about the star from the KIC, tests are performed to search for a difference in even- and odd-numbered event depths. If a significant difference exists, this would suggest that a comparable-brightness EB has been found for which the true period is twice that determined due to the presence of primary and secondary eclipses. Similarly, a search is conducted for evidence of a secondary eclipse or a possible planetary occultation roughly half-way between the potential transits. If a secondary eclipse is seen, then this could indicate that the system is an EB with the period assumed. However, the possibility of a self-luminous planet (as with HAT-P-7; Borucki et al. 2009) must be considered before dismissing a candidate as a false positive.

The shift in the centroid position of the target star measured in and out of the transits must be consistent with that predicted from the fluxes and locations of the target and nearby stars.

After passing these tests, the candidate is elevated to "*Kepler* Object of Interest" (KOI) status and is forwarded to the Threshold Crossing Event Review Team. They examine the information associated with each KOI, add any that they have found by visual inspection, judge the priority of each KOI, and then send the highest priority candidates to the Follow-up Observation Program (FOP) for various types of observations and additional analysis. These observations include the following.

1. High-resolution imaging with adaptive optics or speckle interferometry to evaluate the contribution of other stars to the photometric signal and to evaluate the shift of the photocenter when a transit occurs.
2. Medium-precision RV measurements are made to rule out stellar or brown dwarf mass companions and to better characterize the host star.
3. A stellar blend model (Torres et al. 2004) is used to check that the photometry is consistent with a planet orbiting a star rather than the signature of a multi-star system.
4. High-precision RV measurements may be made, as appropriate, to verify the phase and period of the most promising

candidates and ultimately to determine the mass and eccentricity of the companion and to identify other non-transiting planets. For low-mass planets where the RV precision is not sufficiently high to detect the stellar RV variations, RV observations are conducted to produce an upper limit for the planet mass and assure that there is no other body that could cause confusion.

5. When the observations indicate that the Rossiter–McLaughlin effect (Winn 2007) will be large enough to be measured in the confirmation process, such measurements may be scheduled, typically at the Keck Observatory.
6. When the data indicate the possibility of transit-timing variations large enough to assist in the confirmation process, the multiple-planet and transit-timing working groups perform additional analysis of the light curve and possible dynamical explanations (Steffen et al. 2010).

2.5. Estimate of the False Positive Rate

This paper discusses the characteristics for the 311 candidates (associated with 305 stars) in the released list. These candidates have not been fully vetted through the steps described above, so a substantial fraction of the candidates could be false positives. The process of determining the residual false positive fraction for *Kepler* candidates at various stages in the validation process has not proceeded far enough to make good quantitative statements about the expected true planet fraction, or purity, of the released list but a modest improvement can be made over the broad estimate of 24%–60% good planets given in Gautier et al. (2010).

The candidates come from about 425 TCEs using the first three, pre-FOP, validation steps; i.e., check that the odd- and even-numbered transit depths have the amplitude, search for a secondary eclipse, and check that any centroid shift during the transits is consistent with a transit of the target star. Essentially no analysis of ground-based follow-up observations was applied to the released list. About 29% of the 425 TCEs were removed as false positives, mainly EB target stars and background eclipsing binaries (BGEBs) whose images were confused with those of the target stars. The false positives remaining in the 312 candidates should consist of BGEBs closer to the target star than the preliminary vetting could detect, EBs missed in the preliminary light curve analysis, and triple systems harboring an EB.

The analysis used to identify false positives in the 425 TCEs is not considered thorough. For instance, the centroid motion analysis to detect BGEBs in the released list is not particularly sensitive because only the KIC stars in the aperture used for the KOIs were used. A higher sensitivity to BGEBs is obtained when follow-up imaging of star fields around the KOIs is made using high spatial resolution imaging techniques. A rough estimate is that 70%–90% of the EBs and BGEBs were detected, leaving 14–53 EBs and BGEBs in the list. Analysis of medium-precision RV measurements of 268 of the 400 candidates sequestered by the *Kepler* team shows clear signs of 16 EBs that were not found in a relatively thorough light curve analysis. This fraction implies that 14–22 of these EBs are left in the released list. Brown & Latham (2008) estimate that the number of hierarchical triple systems expected to be seen by the proposed Transiting Exoplanet Survey Satellite (TESS) will be about equal to the number of planets. Almenara et al. (2009) find 6 hierarchical blends and 6 planets in a sample of 49 *CoRoT* candidates that were completely "solved." Combining these estimates yields an expectation of 52 ± 20 EBs and BGEBs in the 312 candidates leaving 249 ± 20 true planets plus hierarchical blends. Assuming a 1:1 ratio of planets to hierarchical blends, the fraction of planets in the released sample is estimated to be 41% ± 7%. This estimate might become as poor as 41% ± 17% if the uncertainty on the 1:1 ratio is as large as 40%, derived from the small number statistics used in the Almenara paper.

It is difficult to compare our estimated purity of 41% to purity estimates of other expolanet surveys at the same stage of candidate vetting. The sample of 49 *CoRoT* candidates in Almenara et al. (2009) is at roughly the same stage of vetting as our sample and yielded 6 planets for a purity of 12%. However, the *Kepler* analysis has been able to take advantage of centroid motion analysis in our vetting while the *CoRoT* sample had essentially no vetting for BGEBs. Reducing the 19 BGEBs in the *CoRoT* sample by 80% to make it similar to our sample produces a purity of 18%. The difference appears to come from the larger fraction of EBs in the *CoRoT* sample than we expect in ours. Estimates for TESS from Brown & Latham (2008) predict 28% purity, near the lower end of estimates for our list at a vetting stage similar to ours.

3. RESULTS

For the released candidates, the KOI number, the KIC number, the stellar magnitude, effective temperature, and surface gravity of the star taken from the KIC are listed in the Appendix. Also listed are the orbital period, epoch, and an estimate of the size of the candidate. When only one transit is seen in the Q1 data, the epoch and period are calculated using data obtained subsequently. More information on the characteristics of each star can be obtained from the KIC. Several of the target stars show more than one series of planetary transit-like events and therefore have more than one planetary candidate. These candidate multi-planet systems are of particular interest to investigations of planetary dynamics. The candidate multiple-planet systems (i.e., KOI 152, 191, 209, 877, and 896) are discussed in a later section.

3.1. Naming Convention

It is expected that many of the candidates listed in the Appendix will be followed up by members of the science community and that many will be confirmed as planets. To avoid confusion in naming them, it is suggested that the community refers to *Kepler* stars as KIC NNNNNNN (with a space between the "KIC" and the number), where the integer refers to the ID in the KIC archived at MAST. For planet identifications, a letter designating the first, second, etc., confirmed planet as "b," "c," etc. should follow the KIC ID number. At regular intervals, the literature will be combed for planets found in the *Kepler* star field, sequential numbers assigned, the IAU-approved prefix ("*Kepler*") added, and the information on the planet with its reference will be placed in the *Kepler* Results Catalog. Preliminary versions of this catalog will be available at the MAST and revised on a yearly basis.

3.2. Statistical Properties of Planet Candidates

We have conducted some statistical analyses of the 306 of the 311 released candidates to investigate the general trends and initial indications of the characteristics of the detected planetary candidates. Five of the 312 candidates were not considered in

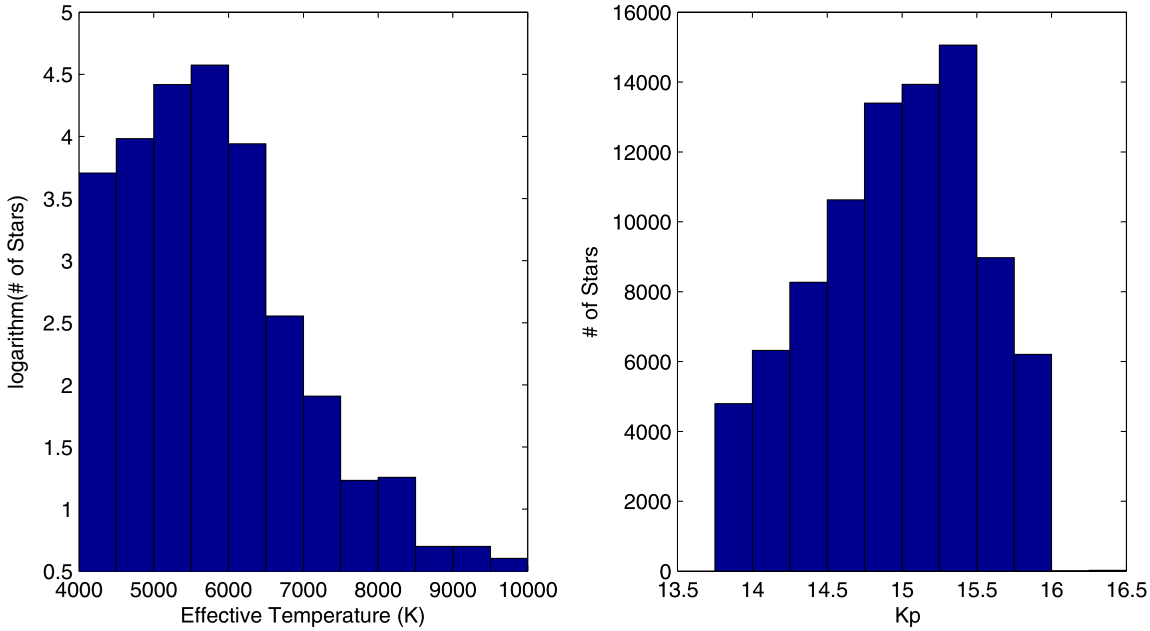

Figure 1. Distributions of effective temperature and magnitude for the stars considered in this study.
(A color version of this figure is available in the online journal.)

the analysis because they were at least twice the size of Jupiter and are likely to be M dwarf stars.

The readers are cautioned that the sample considered here contains many poorly quantified biases. Some of the released candidates could be false positives. Further, those candidates orbiting stars brighter than 13.9 mag and the small-size candidates (i.e., those with radii less than 1.5 $R_{\oplus}$) are not among the released stars. Nevertheless, the large number of candidates provides interesting, albeit tentative, associations with stellar characteristics. Comparisons are limited to orbital periods of <33.5 days. For candidates with periods greater than 16.75 days and that have only a single transit during Q1, data obtained at a later date were used to compute the orbital period to provide necessary information for observers.

In the figures below, the distributions of various parameters are plotted and compared with values in the literature and those derived from the Extrasolar Planets Encyclopedia[28] (EPE; as of 2010 December 7).

The results discussed here for the 306 candidates are primarily based on the observations of 87,615 stars with $K_p > 13.9$ with effective temperature above 4000 K, and with size less than 10 times the size of the Sun. The latter condition is imposed because the photometric precision is insufficient to find Jupiter-size and smaller planets orbiting stars with 100 times area of the Sun. Stellar parameters are based on KIC data. The function of the KIC was to provide a target sample with a low fraction of evolved stars that would be unsuitable for transit work, and to provide a first estimate of stellar parameters that is intended to be refined spectroscopically for KOI at a later time. Spectroscopic observations have not been made for the released stars, so it is important to recognize that some of the characteristics listed for the stars are uncertain, especially surface gravity (i.e., log g) and metallicity ($[M/H]$). The errors in the star diameters can reach 25%, with proportional changes to the estimated diameter of the candidates.

In Figure 1, the stellar distributions of magnitude and effective temperature are given for reference. In later figures, the association of the candidates with these properties is examined.

It is clear from Figure 1 that most of the stars monitored by *Kepler* have temperatures between 4000 and 6500 K; they are mostly late F, G, and K spectral types. This is because these types are the most frequent for a magnitude-limited survey of dwarfs and because the selection of target stars was purposefully skewed to enhance the detectability of Earth-size planets by choosing those with an effective temperature and magnitude that maximized the transit S/N (Batalha et al. 2010). Thus, the decrease in the number of monitored stars for magnitudes greater than 15.5 is due to the selection of only those stars in the field of view (FOV) that are likely to be small enough to show planets. In particular, A, F, and G stars were selected at magnitudes where they are sufficiently bright for their low shot noise to overcome the lower S/N for a given planet size due to their large stellar radii. After all available bright dwarf stars are chosen for the target list, many target slots remain, but only dimmer stars are available (Batalha et al. 2010). From the dimmest stars, the smallest stars are given preference. In the following figures, when appropriate, the results will be based on the ratio of the number of candidates to the number of stars in each category.

A comparison of the distributions shown in Figure 2 indicates that the majority of the candidates discovered by *Kepler* are Neptune-size (i.e., 3.8 $R_{\oplus}$) and smaller; in contrast, the planets discovered by the transit method and listed in the EPE are typically Jupiter-size (i.e., 11.2 $R_{\oplus}$) and larger. This difference is understandable because of the difficulty in detecting small planets when observing through Earth's atmosphere.

The *Kepler* results shown in Figure 2 imply that small candidate planets with periods less than 33.5 days are much more common than large candidate planets with periods less than 33.5 days and that the ground-based discoveries are potentially sampling the upper tail of the size distribution (Gaudi 2005). Note that for a substantial range of planet sizes, an R^{-2}

[28] Extrasolar Planets Encyclopedia: http://exoplanet.eu/.

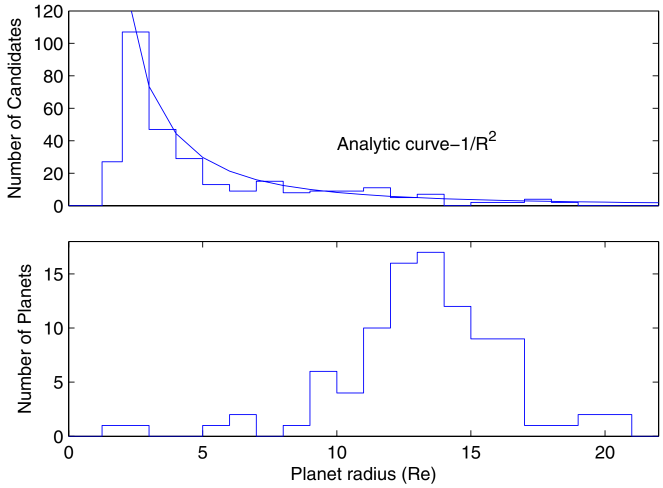

Figure 2. Size distribution. Upper panel: *Kepler* candidates. Lower panel: planets discovered by the transit method and listed in the EPE as of 2010 December 7 (without *Kepler* planets).

(A color version of this figure is available in the online journal.)

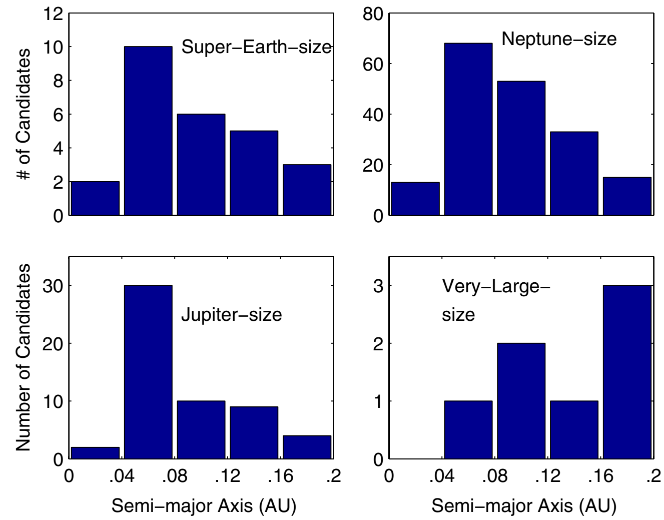

Figure 4. Semi-major axis distribution of candidates grouped into four candidate sizes.

(A color version of this figure is available in the online journal.)

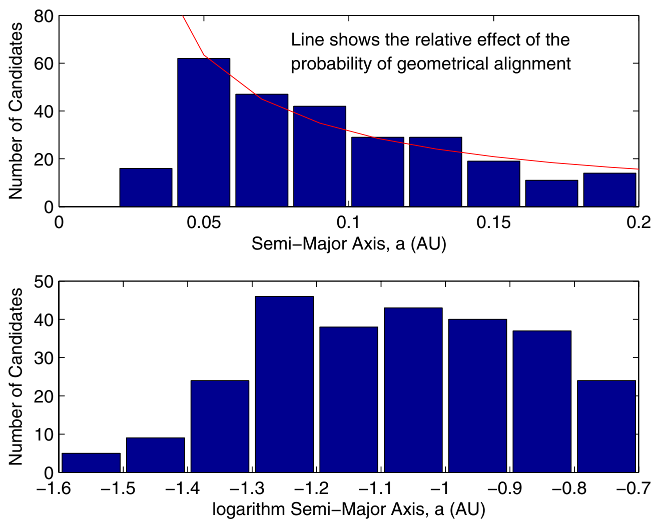

Figure 3. Semi-major axis distribution of candidates. Upper panel: in linear intervals. Lower panel: in logarithmic intervals.

(A color version of this figure is available in the online journal.)

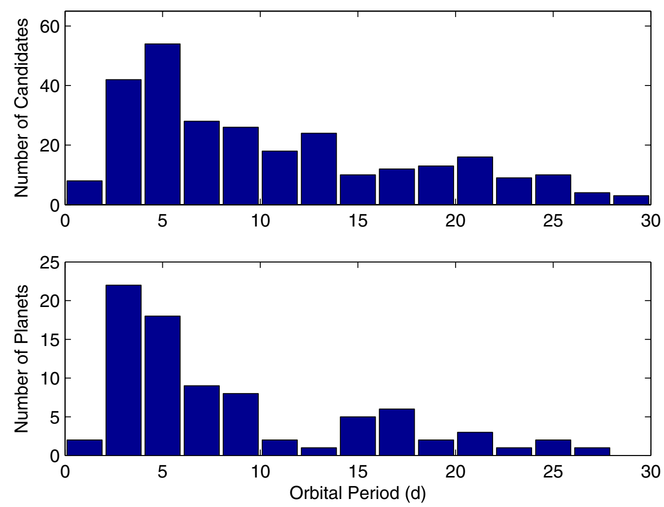

Figure 5. Upper panel: period distribution of *Kepler* candidate planets. Lower panel: period distribution of exoplanets listed in the EPE (as of 2010 December 7) determined from RV measurements.

(A color version of this figure is available in the online journal.)

curve fits the *Kepler* data well. Because it is much easier to detect larger candidates than smaller ones, this result implies that the frequency of planets decreases with the area of the planet, assuming that the false positive rate and other biases are independent of planet size for planets larger than 2 Earth radii.

In Figure 3, the dependence of the number of candidates on the semimajor axis is examined. In the upper panel, an analytic curve has been fitted to show the expected reduction in the integrated number in each interval due to the decreasing geometrical probability that orbits are correctly aligned with the line of sight. It has been fitted over the range of semimajor axis from 0.04 to 0.2 AU corresponding to orbital periods from 3 days to ∼33 days for a solar-mass star.

Although the corrections necessary to normalize the observed distribution to an unbiased one are too lengthy to consider here, we performed a statistical analysis that corrected for the probability of orbital alignment. Although the sample sizes are small and thus the results are uncertain, it is interesting to correct the observations to get a lower limit to the occurrence frequencies.

The corrected number of candidates (Nc) in each 0.01 AU interval of the semimajor axis is estimated from

$$Nc = \text{Average}(a_i/R_i)N_{\text{obs}}, \tag{1}$$

where a_i is the semimajor axis of candidate "i," R_i is the stellar radius of the host star, N_{obs} is the number of detected candidates in the interval of the semimajor axis, and the index "i" counts only those candidates in each increment of the semimajor axis.

Considering only this correction and only for the range of the semimajor axis from 0.04 to 0.2 AU, the fraction of stars detected with candidates is nearly constant with the semimajor axis and equal to 6.8×10^{-2}.

Only a small decrease in the number of candidates with the logarithm of the semimajor axis is seen in the bottom panel of Figure 3. Appropriate corrections for the geometric probability

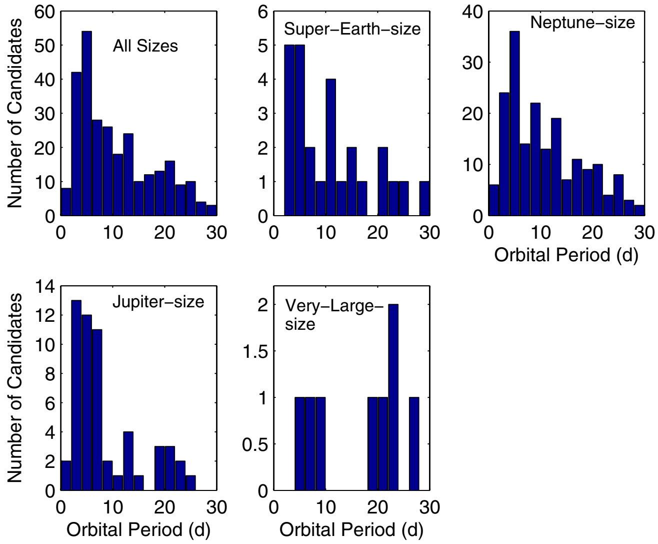

Figure 6. Orbital period distribution for several choices of candidate size.
(A color version of this figure is available in the online journal.)

showed a large increase in the number per logarithmic interval as expected from an examination of the upper panel. Thus, these observations are not consistent with a logarithmic distribution of candidates with semimajor axis.

A breakout of the number of candidates versus semimajor axis is shown in Figure 4. "Super-Earth-size" candidates are those with sizes from 1.25 $R_\oplus$ to 2.0 $R_\oplus$. These are expected to be rocky-type planets without a hydrogen–helium atmosphere. "Neptune-size" candidates are those with sizes from 2.0 $R_\oplus$ to 6 $R_\oplus$, and are expected to be similar to Neptune and the ice giants in composition. Candidates with sizes between 6 and 15 $R_\oplus$ and between 15 and 22 $R_\oplus$ are labeled Jupiter-size and very large candidates, respectively. The nature of the larger category of objects is unclear. No mass measurements are available. It is possible that they are small stars transiting large stars. It is also possible that these are ordinary Jovian planets whose stars have incorrectly assigned radii or that they are the tail of the distribution of large planets.

A correction of these results for the probability of a geometrical alignment shows that the adjusted occurrence frequencies of candidate planets are 8×10^{-3}, 4.6×10^{-2}, 1.2×10^{-2}, and 2×10^{-3} for super-Earth-size, Neptune-size, Jupiter-size, and the very large candidates, respectively. Substantial increases in the values for the smaller candidates are expected when more comprehensive corrections are made for low-level signals that are currently too noisy to produce detectable transits and when a larger range of semimajor axis is considered.

There are several references in the literature to the pile-up of giant planet orbital periods near 3 days (Santos & Mayor 2003) and a "desert" for orbital periods in excess of 5 days. Figure 5 is a comparison of distributions of frequency with orbital period for the *Kepler* results with that derived from the planets listed in the EPE. In this instance, the much larger number of planets listed in the EPE under RV discoveries was used in the comparison. The very compact distribution of frequency with orbital periods between 3 and 7 days seen in the EPE results is also seen in the *Kepler* results. However, there is little sign of the "desert" that has been discussed in the literature with respect to the RV results for giant planets. We note that the *Kepler* sample contains a much larger fraction of super-Earth-size candidates than does the EPE sample.

In Figure 6, the dependences of the number of candidates with the size groups and orbital period are shown.

The first four panels indicate that the observed number of candidates is decreasing with orbital period regardless of size and that there is a peak in concentration for orbital periods between 2 and 5 days for all sizes.

All panels in Figure 7 show a lack of candidates with radius less than 1.5 $R_\oplus$. This result is mostly due to the sequestration of small candidates for follow-up observations during the summer of 2010. In the upper left panel, the decrease in the number of candidates with increasing orbital period and with decreasing size is evident. In contrast to the strong correlation of decreasing

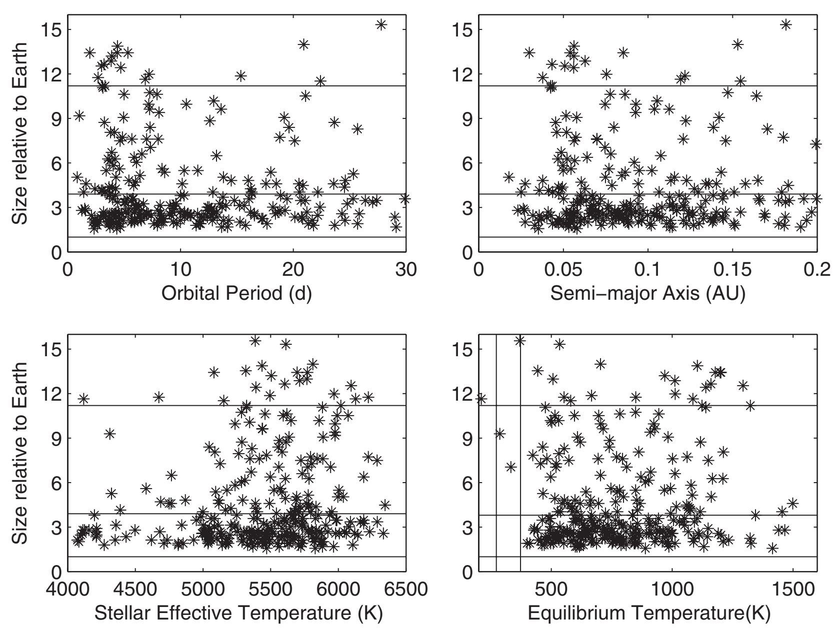

Figure 7. Candidate size vs. orbital period, semimajor axis, stellar effective temperature, and equilibirum temperature. Horizontal lines mark ratios of candidate sizes for Earth-size, Neptune-size, and Jupiter-size relative to Earth size. The vertical lines in panel (d) mark off the HZ temperature range: 273–373 K.

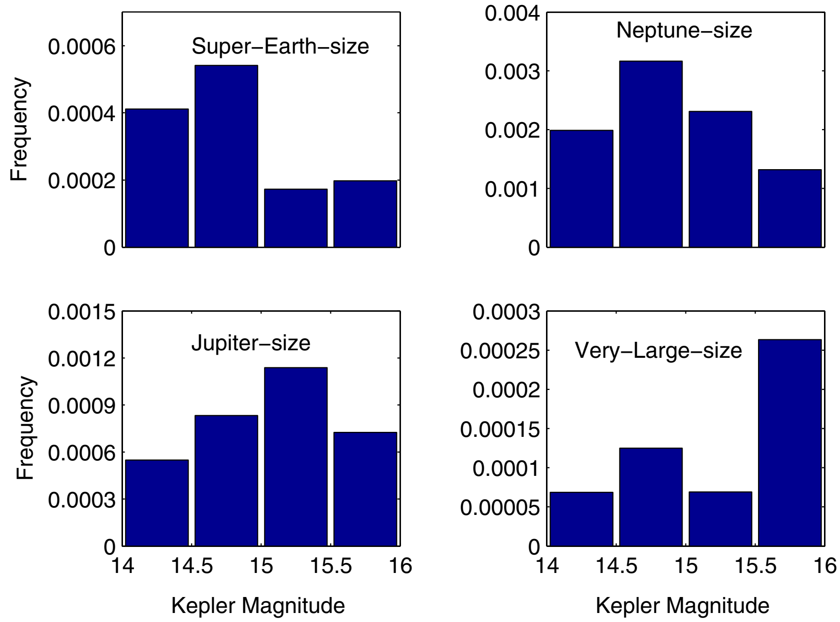

Figure 8. Measured frequencies of candidates for four size ranges as a function of *Kepler* magnitude.
(A color version of this figure is available in the online journal.)

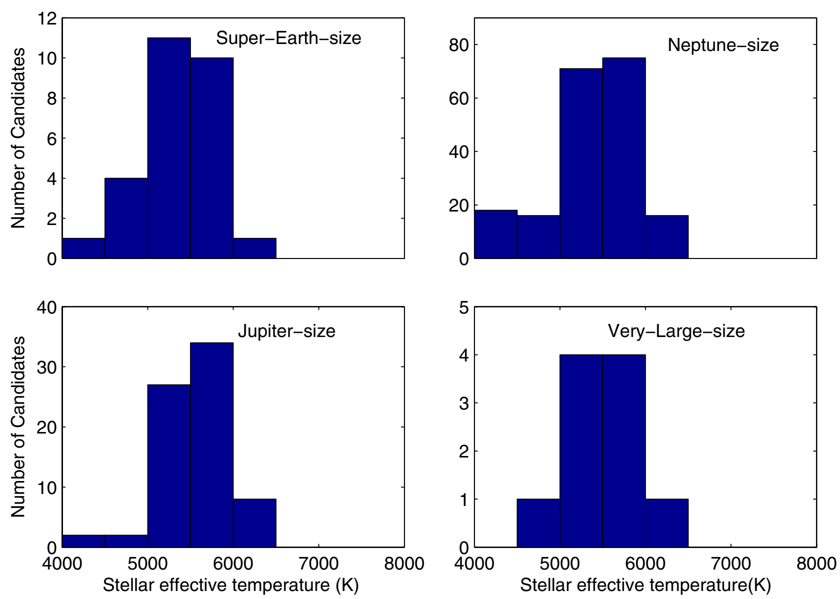

Figure 9. Number of candidates for various candidate sizes vs. stellar effective temperature.
(A color version of this figure is available in the online journal.)

Table 1
Properties of Five Candidates In or Near the HZ

	Candidate Properties				Stellar Properties		
KOI No.	Candidate Size ($R_\oplus$)	Period (days)	T_{eq} (K)	Epoch[a]	KIC No.	T_{eff}[b] (K)	K_p
494.01	1.9	25.698	400	121.780	3966801	4854	14.9
504.01	1.9	40.588	411	132.291	5461440	5403	14.6
819.01	15.6	38.037	370	129.933	4932348	5386	15.5
865.01	7.0	119.021	333	155.237	6862328	5560	15.1
902.01	9.3	83.904	287	169.808	8018547	4312	15.8

Notes.
[a] Epochs are BJD-2454900.
[b] The effective temperatures were derived from spectroscopic observations as described in Steffen et al. (2010).

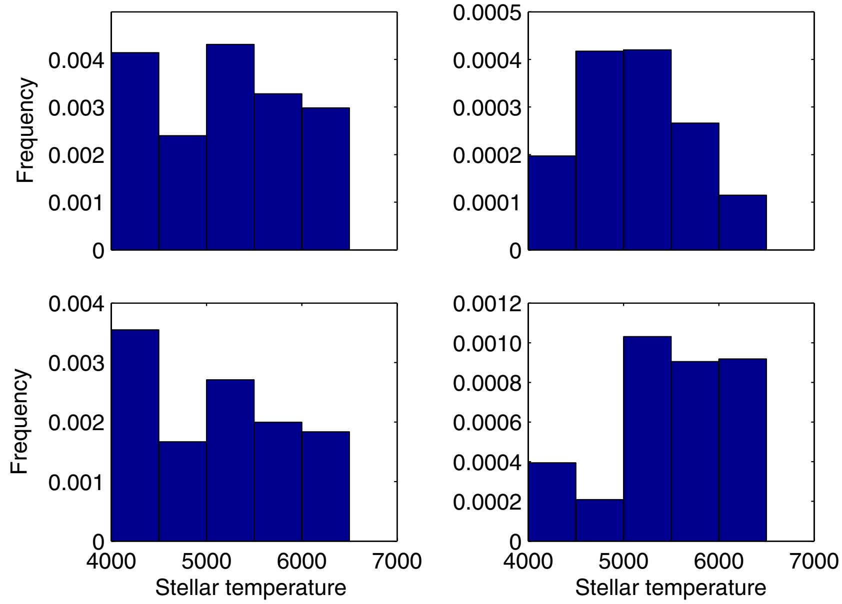

Figure 10. Measured frequency of stars with candidates vs. stellar temperature. From upper left (clockwise): all released candidates, super-Earth-size candidates, Neptune-size candidates, and Jupiter-size candidates.

(A color version of this figure is available in the online journal.)

Table 2
Properties of Five Multi-candidate Systems

Candidate Properties					Stellar Properties			
KOI No,	Candidate Size	Period (days)	Epoch[a]	KIC No.	$T_{\rm eff}$[b] (K)	K_p	R.A. (2000)	Decl.
152.01	0.58 R_J	>27	91.747	8394721	6500	13.9	20 02 04.1	44 22 53.7
152.02	0.31 R_J	27.41	66.630					
152.03	0.30 R_J	13.48	69.622					
191.01	1.06 R_J	15.36	65.385	5972334	5500	15.0	19 41 08.9	41 13 19.1
191.02	2.04 $R_\oplus$	2.42	65.50					
209.01	1.05 R_J	>29	68.635	10723750	6100	14.2	19 15 10.3	48 02 24.8
209.02	0.68 R_J	18.80	78.822					
877.01	2.53 $R_\oplus$	5.95	103.956	7287995	4500	15.0	19 34 32.9	42 49 29.9
877.02	2.34 $R_\oplus$	12.04	114.227					
896.01	0.38 R_J	16.24	108.568	7825899	5000	15.3	19 32 14.9	43 34 52.9
896.02	0.28 R_J	6.31	107.051					

Notes.
[a] Epochs are BJD-2454900.
[b] The effective temperatures were derived from spectroscopic observations as described in Steffen et al. (2010).

planet mass with orbital period found by Torres et al. (2008), no analogous dependence of candidate size with orbital period is evident.

The vertical lines in the bottom right panel mark the edges of the HZ; i.e., temperatures of 273 and 373 K. The equilibrium temperatures for the candidates were computed for a Bond albedo of 0.3 and a uniform surface temperature. However, the computed temperatures have an uncertainty of approximately ±50 K, because of the uncertainties in the stellar size, mass, and temperature as well as the effect of any atmosphere. Over this wider temperature range, five candidates are present; two near super-Earth size, and three bracketing the size of Jupiter; see Table 1.

In Figure 8, the frequency of candidates in each magnitude bin has been calculated from the number of candidates in each bin divided by the total number of stars monitored in each bin. The number of stars brighter than 14.0 mag and fainter than 16.0 in the current list is so small that the count is not shown.

The panel for super-Earth-size candidates shows a substantial decrease in frequency for magnitudes larger than 15.0 and is indicative of difficulty in detecting small candidates around dim stars.

Figure 9 shows that the number of candidates is a maximum for stars with temperatures between 5000 and 6000 K, i.e., G-type dwarfs. This result should be expected because a large number of G -type stars are chosen as target stars. The relatively large number of super-Earth- and Neptune-size candidates orbiting K stars (4000 K $\leqslant$ stellar temperature $\leqslant$ 5000 K) is likely the result of small planets being easier to detect around small stars than around large stars and the relatively large number of such stars chosen. Similarly, the paucity of candidates associated with stars at temperatures above 6000 K is likely to be due to the relatively small number of such stars in the survey.

In Figure 10, the bias associated with the number of target stars monitored as a function of temperature is removed by

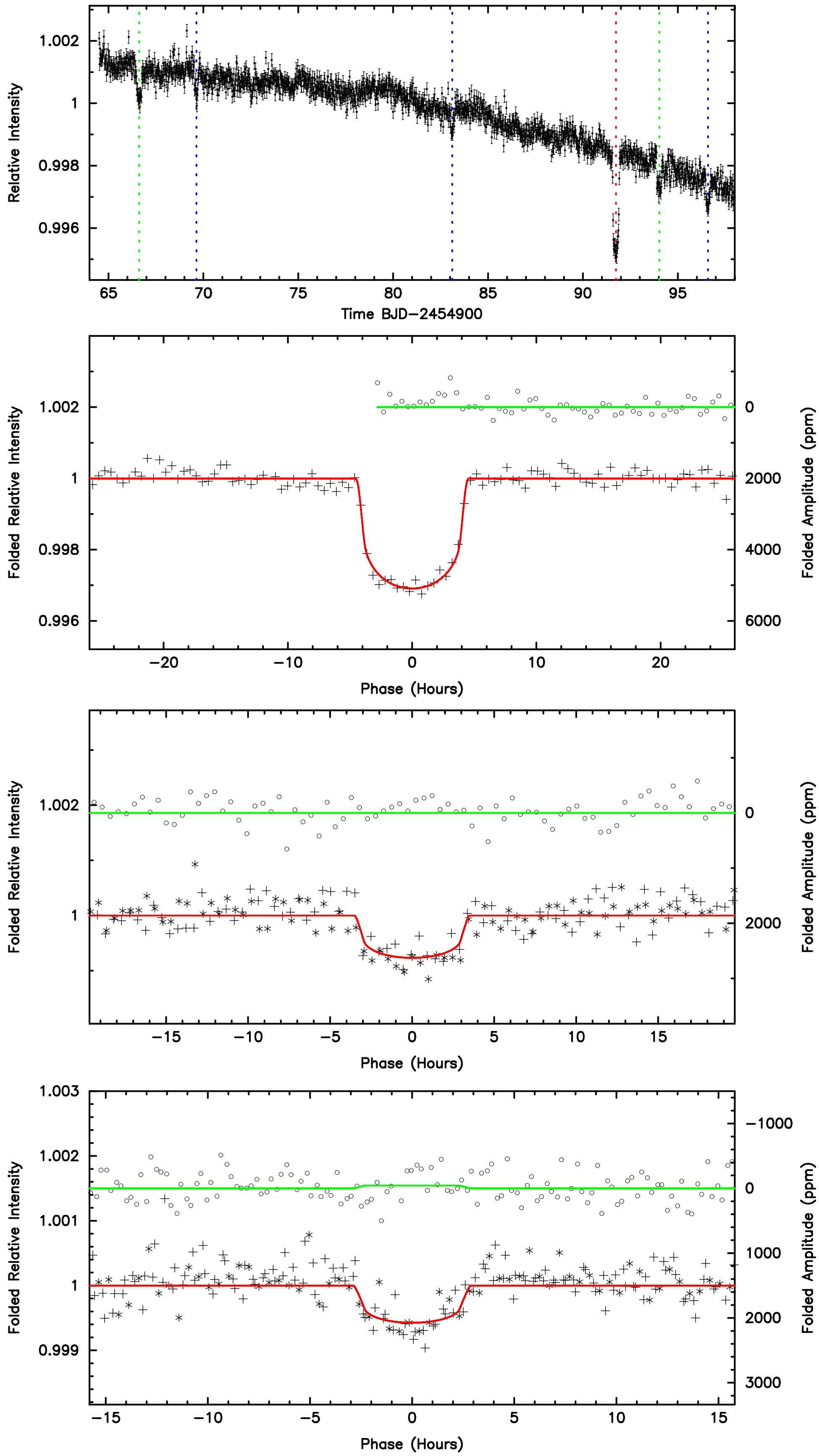

Figure 11. Three candidate planets associated with KIC 8394721. The position of the vertical dotted lines shows the position of the transits observed for each of the candidates.

(A color version of this figure is available in the online journal.)

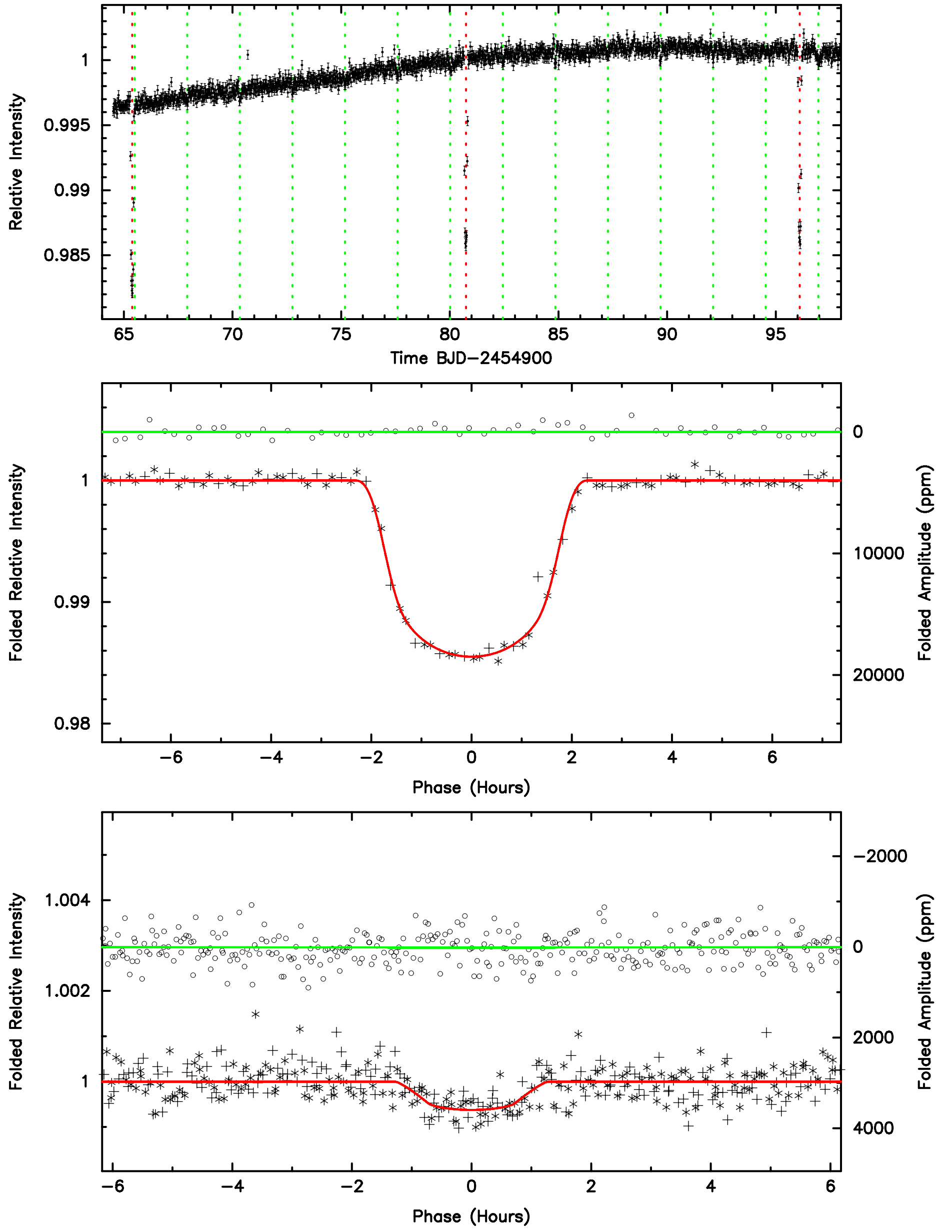

Figure 12. Two candidate planets associated with KIC 5972334. The clear detection of two candidates (1.06 R_J and 2.0 $R_\oplus$) demonstrates that *Kepler* can detect super-Earth-size candidates even for stars as dim as 15th magnitude.

(A color version of this figure is available in the online journal.)

computing the frequencies of the candidates as a fraction of the number of stars monitored.

Note that the frequency for the total of all candidate sizes is nearly constant with increasing stellar temperature. However, for super-Earth candidates, the decrease with temperature is quite marked, as might be expected when considering the substantially lower S/N due to the increase of stellar size of main-sequence stars with temperature. It is unclear whether the decrease in occurrence frequency is real or a measurement bias. The observed increase in the frequency with stellar temperature for Jupiter-size candidates should not be biased because the signal level for such large candidates is many times the noise level associated with the instrument and shot noise. Thus, this increase could indicate a real, positive correlation of giant candidates with stellar mass (Johnson et al. 2010).

A study of the dependence of the frequency of the planet candidates on the stellar metallicity was not considered, because the metallicities in the KIC are not considered sufficiently reliable. In particular, the D51 filter used in the estimation of metallicity is sensitive to a combination of the effects of surface gravity and metallicity, especially within the temperature range from roughly late K to late F stars. However, the information generated by this filter was used to develop the association with log g, thereby making any estimate of metallicity highly uncertain.

4. EXAMPLES OF CANDIDATE MULTI-PLANET SYSTEMS

A number of target stars with multiple-planet candidates orbiting a single star have been detected in the *Kepler* data. The light curves for five multi-candidate systems in the released data are shown in Figures 11–15. Only a single transit-like event is seen in Q1 for some planet candidates, as expected for planets

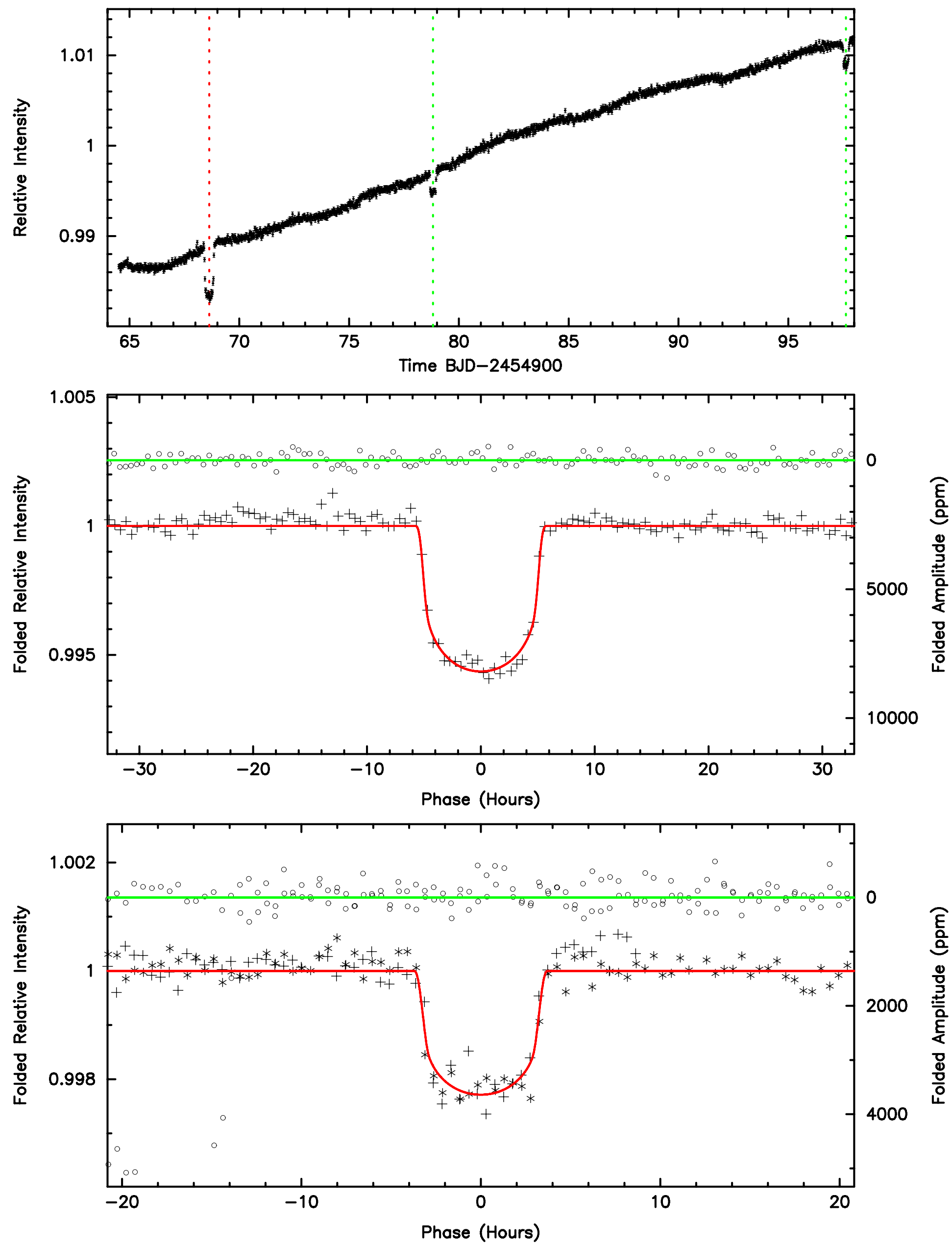

Figure 13. KIC 10723750. The two sets of transits correspond to two different Jupiter-size (1.05 and 0.68 R_J) candidates with long periods.
(A color version of this figure is available in the online journal.)

with orbital periods exceeding the 33.5 days of observations. For other candidate systems, several transits of multiple-planet candidates have been observed.

In two cases, the ratio of putative orbital periods is near 2. For such a system there is a high (60%) conditional probability that both planets transit, provided that the inner planet transits and the system is planar. For systems with planet candidates having a large ratio of orbital periods (e.g., KOI 191), the probability that the outer planet will transit, given that the inner one does, is small. While an exhaustive study remains to be done, the implication is that many planetary systems have multiple planets or that nearly coplanar planetary systems might be common.

Any of these multiple-planet candidate systems, as well as the single-planet candidate systems, could harbor additional planets that do not transit and therefore are not seen in these data. Such planets might be detectable via transit-timing variations of the transiting planets after several years of *Kepler* photometry (Agol et al. 2005; Holman & Murray 2005). Based on the data presented here, we do not find any statistically significant transit-timing variations for the five candidate multiple-planet systems or for the single-planet candidates listed in the Appendix.

Table 2 lists the general characteristics of the five multi-candidate systems in the released data. It should be noted that in previous instances, multiple EBs have been seen in the same photometric aperture and can appear to be multiple-planet systems. A thorough analysis of each system and a check for background binaries are required before any discovery should be claimed. A more extensive discussion of these candidates can be found in Steffen et al. (2010).

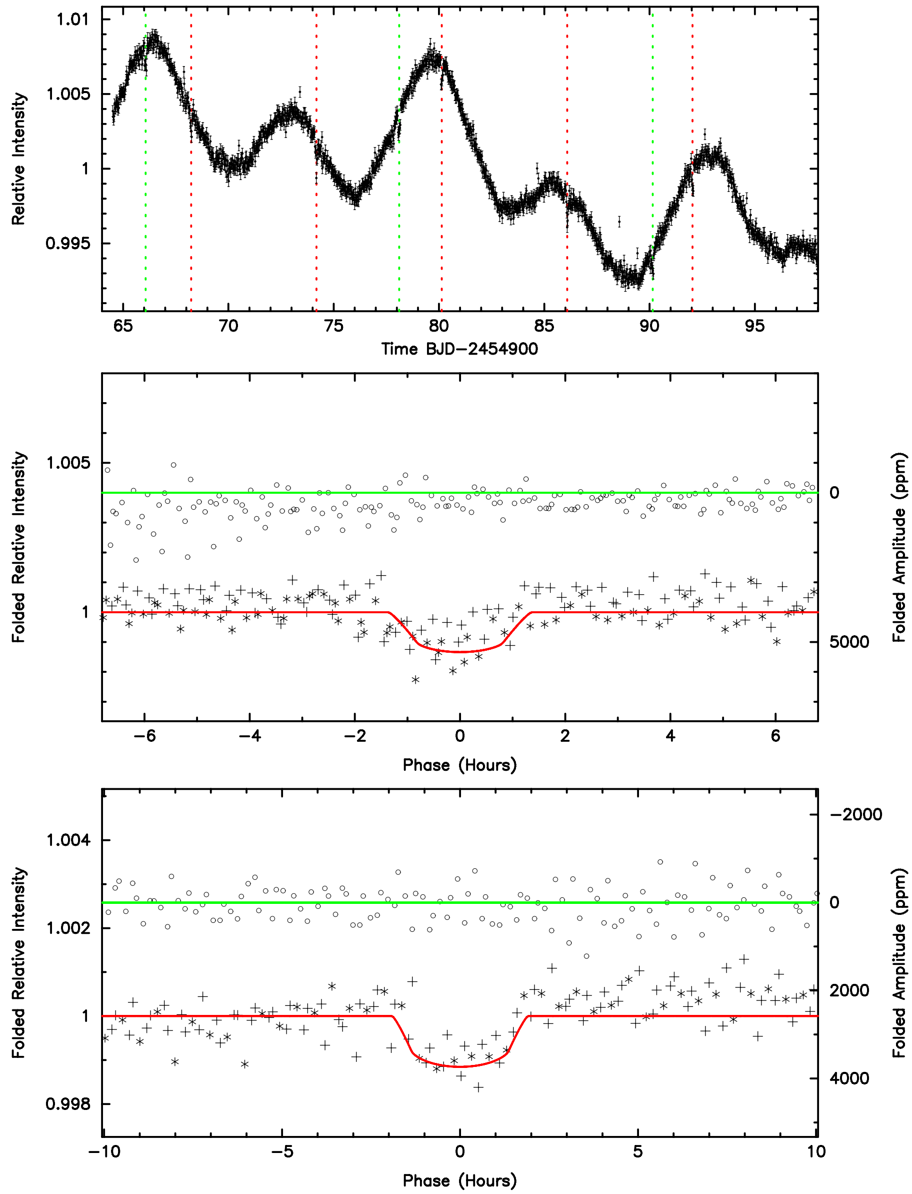

Figure 14. KIC 7287995. A cool, spotted star with two super-Earth candidates (2.7 and 2.3 $R_{\oplus}$) with near-resonant periods of 5.96 and 12.04 days.
(A color version of this figure is available in the online journal.)

5. ECLIPSING BINARY DATA

More than 1.2% of *Kepler* stars are EB stars. Statistical results derived from 1832 EBs are presented by Prsa et al. (2010). Figure 16 depicts a distribution of EB periods. The stacked gray-scaled bars correspond to different morphologic types. This distribution can be readily compared to that for transiting planets shown in Figure 5 for the planetary candidates. The distribution of observed EB stars is more heavily weighted toward short periods than is the distribution of planet candidates. This is due to over-contact binaries and ellipsoidal variables, for which there is no counterpart among planets. For a comprehensive discussion of EB stars seen in the *Kepler* data, see Prsa et al. (2010).

6. SUMMARY AND CONCLUSIONS

The following conclusions must be tempered by recognizing that many sources of bias exist in the results and that the results apply only to the released candidates.

Most candidate planets are less than half the radius of Jupiter.

Five candidates are present in and near the HZ; two near super-Earth size, and three bracketing the size of Jupiter.

There is a narrow maximum in the frequency of candidates with orbital period in the range from 2 to 5 days. This peak is more prominent for large candidate planets than for small candidates.

The adjusted occurrence frequencies of super-Earth-, Neptune-, Jupiter-, and very large size candidates in short-period orbits are approximately 8×10^{-3}, 4.6×10^{-2}, 1.2×10^{-2}, and 2×10^{-3}, respectively. These values are expected to be lower than unbiased values because no corrections have been made for factors such as stellar magnitude and variability which have substantial effects on the detectability.

The distributions of orbital period and magnitude of the candidates much larger than Jupiter appear to be quite different from those of smaller candidates and might represent small stellar companions or errors in the size estimation of the dimmest stars in the *Kepler* planet search program.

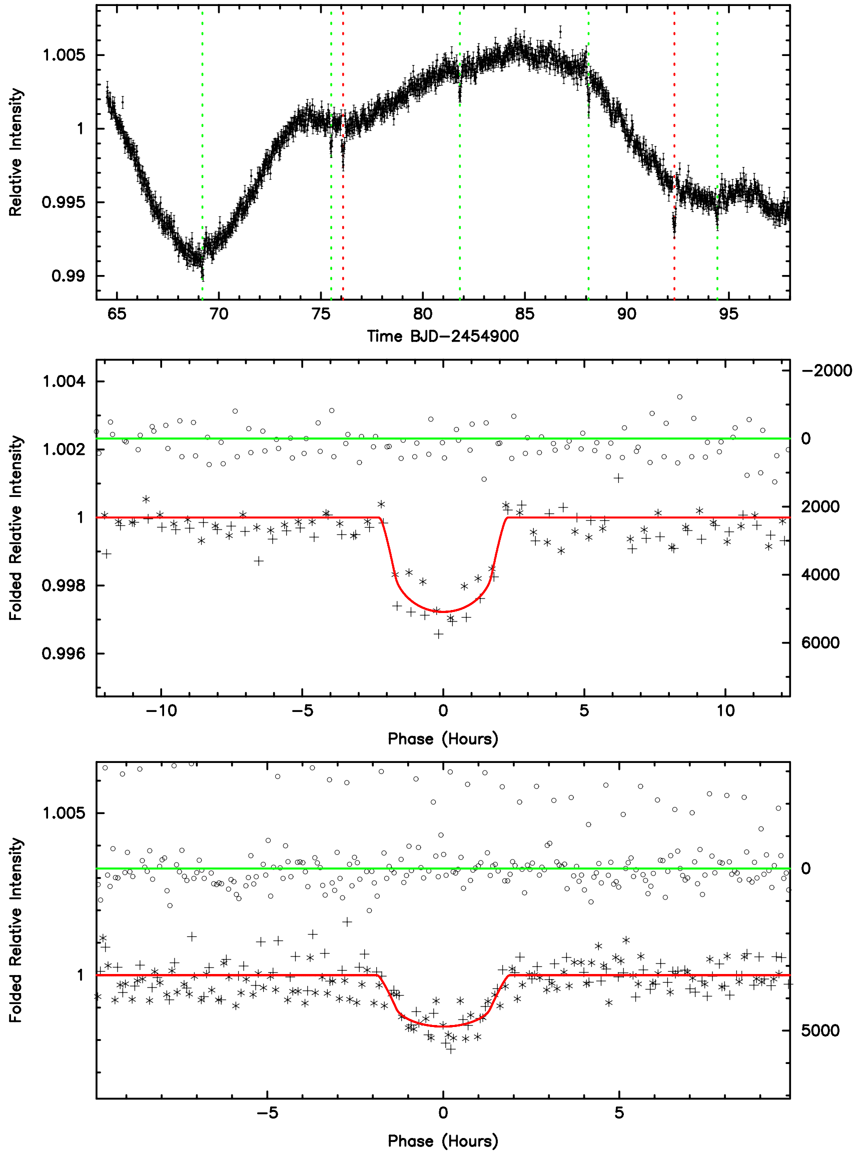

Figure 15. KIC 7825899. A K-type star with two Neptune-size candidates in 6.3-day and 16.2-day orbits.
(A color version of this figure is available in the online journal.)

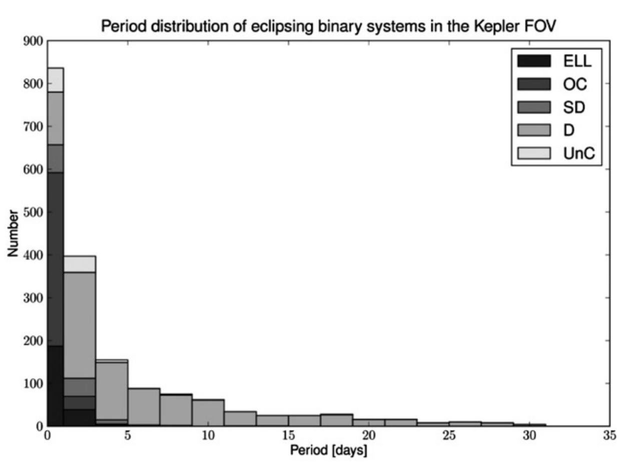

Figure 16. Distribution of EB stellar periods. Objects are classified into five groups based on their morphologic type: ellipsoidal variables (ELL), overcontact binaries (OC), semi-detached binaries (SD), detached binaries (D), and uncertain (UnC).

One of the five candidate multi-planet systems has two super-Earth-size candidates (2.5 and 2.3 $R_\oplus$) with near-resonant periods of 5.96 and 12.04 days.

Kepler was competitively selected as the 10th Discovery mission. Funding for this mission is provided by NASA's Science Mission Directorate. Some of the data presented herein were obtained at the W. M. Keck Observatory, which is operated as a scientific partnership among the California Institute of Technology, the University of California, and the National Aeronautics and Space Administration. The Observatory was made possible by the generous financial support of the W. M. Keck Foundation. The authors thank the many people who gave so generously of their time to make this mission a success.

APPENDIX

For the released candidates, the KOI number, the KIC number, the stellar magnitude, effective temperature, and surface gravity of the star taken from the KIC are listed in Table A1. Also listed

Table A1
List of Planetary Candidates

KOI	KIC Number	*Kp*	Planet Radius R_J	Epoch BJD-2454900	Period (days)	T_{eff} (K)	log(*g*) (cgs)	$R*$ (Sun)
152.01	8394721	13.9	0.57	91.750	52.088	6187	4.536	0.936
152.02	8394721	13.9	0.31	66.634	27.401	6187	4.536	0.936
152.03	8394721	13.9	0.29	69.622	13.484	6187	4.536	0.936
191.01	5972334	15.0	1.06	65.385	15.359	5495	4.519	0.921
191.02	5972334	15.0	0.19	65.492	2.419	5495	4.519	0.921
209.01	10723750	14.3	1.05	68.635	50.789	6221	4.478	1.418
209.02	10723750	14.3	0.69	78.821	18.796	6221	4.478	1.418
184.01	7972785	14.9	1.59	66.566	7.301	6134	4.431	1.534
187.01	7023960	14.9	1.16	84.529	30.883	5768	4.703	0.829
188.01	5357901	14.7	0.72	66.508	3.797	5087	4.730	0.681
193.01	10799735	14.9	1.46	90.349	37.590	5883	4.465	1.008
194.01	10904857	14.8	0.99	72.466	3.121	5883	4.633	0.820
195.01	11502867	14.8	1.13	66.630	3.218	5604	4.498	0.955
198.01	10666242	14.3	3.43	86.369	87.233	5538	4.629	0.806
200.01	6046540	14.4	0.63	67.344	7.341	5774	4.690	0.759
204.01	9305831	14.7	0.78	66.379	3.247	5287	4.476	1.043
206.01	5728139	14.5	1.20	64.982	5.334	5771	4.345	1.904
208.01	3762468	15.0	1.12	67.710	3.004	6094	4.585	1.176
210.01	10602291	14.9	1.25	72.326	20.927	5812	4.352	1.154
211.01	10656508	15.0	0.94	69.014	35.875	6072	4.407	1.091
212.01	6300348	14.9	0.68	72.231	5.696	5843	4.538	1.056
214.01	11046458	14.3	1.00	64.741	3.312	5322	4.442	0.999
215.01	12508335	14.7	2.70	88.206	42.944	5535	4.395	1.078
217.01	9595827	15.1	1.18	66.414	3.905	5504	4.724	0.896
219.01	6305192	14.2	0.68	65.470	8.025	5347	4.727	1.372
220.01	7132798	14.2	0.38	65.939	2.422	5388	4.867	0.989
221.01	3937519	14.6	0.49	65.441	3.413	5176	4.686	0.898
223.01	4545187	14.7	0.24	67.478	3.177	5128	4.657	0.744
224.01	5547480	14.8	0.32	65.073	3.980	5740	4.507	0.951
225.01	5801571	14.8	0.45	74.537	0.839	6037	4.546	0.919
226.01	5959753	14.8	0.22	71.116	8.309	5043	4.892	0.869
229.01	3847907	14.7	0.56	67.934	3.573	5608	4.370	1.119
234.01	8491277	14.3	0.29	65.187	9.614	5735	4.356	1.205
235.01	8107225	14.4	0.18	66.818	5.632	5041	4.654	0.740
237.01	8041216	14.2	0.20	67.788	8.508	5679	4.533	0.919
239.01	6383785	14.8	0.31	71.556	5.641	5983	4.539	0.924
240.01	8026752	15.0	0.45	71.615	4.287	5996	4.602	1.446
241.01	11288051	14.1	0.19	64.796	13.821	5055	4.854	0.689
242.01	3642741	14.7	0.86	71.343	7.259	5437	4.507	1.556
403.01	4247092	14.2	1.58	104.132	21.057	5565	4.440	1.022
409.01	5444548	14.2	0.21	112.522	13.249	5709	5.008	0.993
410.01	5449777	14.5	1.07	109.286	7.217	5968	4.384	1.117
412.01	5683743	14.3	0.72	103.325	4.147	5584	4.275	1.256
413.01	5791986	14.8	0.28	109.558	15.229	5236	4.557	8.560
416.01	6508221	14.3	0.27	118.841	18.208	5083	4.647	0.750
417.01	6879865	14.8	0.81	109.965	19.193	5635	4.594	0.851
418.01	7975727	14.5	1.03	105.796	22.418	5153	4.422	1.010
419.01	8219673	14.5	0.67	122.391	20.131	5723	4.695	0.752
420.01	8352537	14.2	0.42	107.084	6.010	4687	4.513	0.831
421.01	9115800	15.0	1.60	105.819	4.454	5181	4.317	1.158
423.01	9478990	14.3	0.94	135.857	21.087	5992	4.448	1.138
425.01	9967884	14.7	0.43	102.753	5.428	5689	4.544	0.438
426.01	10016874	14.7	0.36	105.152	16.301	5796	4.328	1.188
427.01	10189546	14.6	0.43	124.737	24.615	5293	4.496	0.930
428.01	10418224	14.6	1.04	105.518	6.873	6127	4.549	1.927
429.01	10616679	14.5	0.48	105.527	8.600	5093	4.485	1.024
430.01	10717241	14.9	0.25	112.402	12.377	4124	4.584	0.640
431.01	10843590	14.3	0.34	111.712	18.870	5249	4.433	1.004
432.01	10858832	14.3	0.32	107.350	5.263	5830	4.457	1.015
433.01	10937029	14.9	0.52	104.095	4.030	5237	4.372	1.084
434.01	11656302	14.6	1.69	106.103	22.265	5172	4.564	1.350
435.01	11709124	14.5	0.36	111.951	20.548	5709	4.663	1.039
438.01	12302530	14.3	0.19	107.796	5.931	4351	4.595	0.679
441.01	3340312	14.5	0.24	106.917	30.544	6231	4.628	0.838
443.01	3833007	14.2	0.24	113.046	16.217	5614	4.617	1.020

Table A1
(Continued)

KOI	KIC Number	Kp	Planet Radius R_J	Epoch BJD-2454900	Period (days)	T_{eff} (K)	log(g) (cgs)	$R*$ (Sun)
450.01	6042214	14.2	0.30	104.953	27.047	6089	4.561	0.904
451.01	6200715	14.9	0.23	105.178	3.724	6333	4.648	1.012
452.01	6291033	14.6	0.34	102.939	3.706	5935	4.409	1.771
454.01	7098355	14.8	0.21	103.557	29.007	5138	4.569	0.835
456.01	7269974	14.6	0.27	104.476	13.700	5644	4.515	0.950
457.01	7440748	14.2	0.19	107.295	4.921	4931	4.650	0.729
458.01	7504328	14.7	0.94	141.081	53.717	5593	4.280	1.248
459.01	7977197	14.2	0.32	103.102	19.447	5601	4.428	1.040
460.01	8043638	14.7	0.41	109.077	17.587	5387	4.334	1.150
466.01	9008220	14.7	0.28	103.538	9.391	5907	4.896	0.590
467.01	9583881	14.8	0.48	115.442	18.009	5583	4.539	0.979
468.01	9589524	14.8	0.36	107.596	22.184	4999	4.499	0.900
469.01	9703198	14.7	0.49	107.607	10.329	6005	4.631	0.827
470.01	9844088	14.7	0.35	104.150	3.751	5542	4.653	0.782
471.01	10019643	14.4	0.17	104.730	21.348	5548	4.670	0.766
472.01	10123064	15.0	0.38	106.565	4.244	5682	4.580	1.149
473.01	10155434	14.7	0.22	113.637	12.705	5379	4.686	0.737
474.01	10460984	14.3	0.22	109.721	10.946	6143	4.468	1.015
476.01	10599206	15.0	0.23	111.437	18.428	4993	4.514	0.881
477.01	10934674	14.7	0.23	102.646	16.542	5039	4.513	0.889
480.01	11134879	14.3	0.24	105.308	4.302	5324	4.511	0.915
482.01	11255761	14.9	0.30	102.552	4.993	5526	4.426	1.036
483.01	11497977	14.7	0.23	106.257	4.799	5410	4.703	0.938
484.01	12061222	14.5	0.20	108.064	17.204	5065	4.759	0.745
486.01	12404305	14.1	0.22	102.492	22.184	5625	5.000	0.969
487.01	12834874	14.5	0.17	106.036	7.659	5463	4.510	0.977
488.01	2557816	14.7	0.18	109.444	9.380	5488	4.490	0.955
491.01	3541800	14.4	0.15	102.670	4.662	5965	4.684	0.798
492.01	3559935	14.4	0.32	127.712	29.910	5373	4.263	1.258
493.01	3834360	14.7	0.21	103.125	2.908	5583	4.571	0.871
494.01	3966801	14.9	0.17	121.780	25.698	4854	4.904	0.620
497.01	4757437	14.6	0.24	108.609	13.193	6045	4.495	1.163
499.01	4847534	14.3	0.17	107.535	9.669	5362	4.531	0.896
501.01	4951877	14.6	0.29	103.340	24.793	5556	4.501	1.502
502.01	5282051	14.3	0.18	104.159	5.910	5288	4.339	1.134
503.01	5340644	15.0	0.23	105.958	8.222	4110	4.550	0.673
504.01	5461440	14.6	0.17	132.291	40.588	5403	4.754	0.678
505.01	5689351	14.2	0.33	107.812	13.767	4985	4.242	1.259
506.01	5780715	14.7	0.25	102.966	1.583	5777	4.557	0.896
507.01	5812960	14.9	0.41	106.494	18.495	5117	4.408	1.024
509.01	6381846	14.9	0.23	102.712	4.167	5437	4.565	0.900
511.01	6451936	14.2	0.25	103.504	8.006	5802	4.404	1.083
512.01	6838050	14.8	0.25	105.919	6.510	5406	4.316	1.178
513.01	6937692	14.9	0.30	103.098	35.181	6288	4.577	1.204
514.01	7602070	14.4	0.17	109.061	11.757	5446	4.916	0.841
519.01	8022244	14.9	0.21	111.337	11.904	5807	4.523	0.991
520.01	8037145	14.6	0.26	103.304	12.760	5048	4.465	0.946
521.01	8162789	14.6	0.41	105.003	10.161	5767	4.394	1.094
522.01	8265218	14.4	0.19	102.940	12.831	5663	4.910	0.631
523.01	8806123	15.0	0.63	131.230	49.413	5942	4.421	1.066
524.01	8934495	14.9	0.20	104.997	4.593	5187	4.698	0.720
525.01	9119458	14.5	0.49	106.678	11.532	5524	4.281	1.241
526.01	9157634	14.4	0.22	104.044	2.105	5467	4.633	0.796
528.01	9941859	14.6	0.29	109.674	9.577	5448	4.346	1.138
532.01	10454313	14.7	0.23	106.689	4.222	5874	4.540	1.033
533.01	10513530	14.7	0.22	104.698	16.550	5198	4.444	0.985
535.01	10873260	14.4	0.40	104.182	5.853	5782	4.450	1.358
537.01	11073351	14.7	0.18	103.785	2.820	5889	4.906	0.949
538.01	11090765	14.6	0.24	104.657	21.214	5923	4.427	1.061
539.01	11246364	14.1	0.15	104.196	29.122	5722	4.361	1.137
540.01	11521048	14.9	0.74	127.824	25.703	5361	4.498	0.934
541.01	11656721	14.7	0.15	113.347	13.647	5369	4.712	0.741
542.01	11669239	14.3	0.24	111.682	41.889	5509	4.357	1.128
543.01	11823054	14.7	0.17	106.438	4.302	5166	4.724	0.686
544.01	11913012	14.8	0.15	104.669	3.748	5883	4.585	1.012

Table A1
(Continued)

KOI	KIC Number	*Kp*	Planet Radius R_J	Epoch BJD-2454900	Period (days)	T_{eff} (K)	log(*g*) (cgs)	$R*$ (Sun)
546.01	12058931	14.9	0.31	103.186	20.686	5989	4.487	1.244
547.01	12116489	14.8	0.32	121.061	25.302	5086	4.619	0.788
549.01	3437776	14.6	0.44	126.512	42.895	5609	4.414	1.059
551.01	4270253	14.9	0.17	111.850	11.636	5627	4.667	0.775
552.01	5122112	14.7	1.00	104.099	3.055	6018	4.431	1.057
553.01	5303551	14.9	0.20	104.453	2.399	5404	4.394	1.140
554.01	5443837	14.5	0.39	103.544	3.658	5835	4.641	0.809
557.01	5774349	15.0	0.28	103.785	15.656	5002	4.415	1.005
558.01	5978361	14.9	0.22	106.084	9.179	5281	4.580	0.835
559.01	6422367	14.8	0.17	106.712	4.330	5187	4.467	0.955
560.01	6501635	14.7	0.16	112.266	23.678	5142	4.834	0.750
563.01	6707833	14.5	0.18	108.632	15.284	5879	4.477	1.173
564.01	6786037	14.9	0.31	104.887	21.060	5686	4.525	1.453
565.01	7025846	14.3	0.14	103.202	2.340	5829	4.409	1.068
569.01	8008206	14.5	0.21	118.442	20.725	5039	4.546	0.851
570.01	8106610	14.8	0.27	105.782	12.399	6079	4.452	1.033
572.01	8193178	14.2	0.23	112.777	10.640	5666	4.310	1.325
573.01	8344004	14.7	0.28	105.505	5.997	5729	4.352	1.149
574.01	8355239	14.9	0.21	104.362	20.136	5047	4.669	0.727
575.01	8367113	14.7	0.23	116.405	24.321	5979	4.480	0.994
578.01	8565266	14.7	0.46	102.879	6.413	5777	4.362	1.528
580.01	8625925	14.9	0.19	108.711	6.521	5603	4.920	0.806
581.01	8822216	14.8	0.23	108.914	6.997	5514	4.856	0.761
582.01	9020160	14.8	0.20	103.467	5.945	5103	4.650	0.750
583.01	9076513	14.6	0.17	103.740	2.437	5735	4.550	1.197
585.01	9279669	14.9	0.18	104.558	3.722	5437	4.737	0.695
586.01	9570741	14.6	0.16	108.979	15.779	5707	4.669	0.802
587.01	9607164	14.6	0.28	104.606	14.034	5112	4.423	1.005
588.01	9631762	14.3	0.21	108.672	10.356	4431	4.459	0.852
590.01	9782691	14.6	0.16	107.545	11.389	6106	4.546	0.922
592.01	9957627	14.3	0.24	108.475	39.759	5810	4.408	1.077
593.01	9958962	15.0	0.19	104.792	9.997	5737	4.617	0.889
597.01	10600261	14.9	0.20	109.942	17.308	5833	4.416	1.046
598.01	10656823	14.8	0.18	104.152	8.309	5171	4.811	0.749
599.01	10676824	14.9	0.20	106.212	6.455	5820	4.540	0.916
600.01	10718726	14.8	0.18	103.367	3.596	5869	4.445	1.032
602.01	12459913	14.6	0.23	110.276	12.914	6007	4.405	1.282
605.01	4832837	14.9	0.16	102.718	2.628	4270	4.757	0.581
607.01	5441980	14.4	0.57	106.492	5.894	5497	4.608	0.825
608.01	5562784	14.7	0.47	125.921	25.333	4324	4.551	1.326
609.01	5608566	14.5	1.20	105.027	4.397	5696	4.295	1.231
610.01	5686174	14.7	0.19	113.850	14.281	4072	4.529	0.687
614.01	7368664	14.5	0.36	103.023	12.875	5675	4.887	0.589
617.01	9846086	14.6	2.06	131.599	37.865	5594	4.530	0.917
618.01	10353968	15.0	0.28	111.347	9.071	5471	4.516	0.922
620.01	11773022	14.7	0.65	92.107	45.154	5803	4.544	1.384
725.01	10068383	15.8	0.75	102.644	7.305	5046	4.652	0.882
726.01	10157573	15.1	0.30	106.266	5.116	6164	4.508	0.969
728.01	10221013	15.4	0.89	103.121	7.189	5976	4.544	0.918
729.01	10225800	15.6	0.36	102.674	1.424	5707	4.608	0.838
730.01	10227020	15.3	0.31	109.793	14.785	5599	4.386	1.287
732.01	10265898	15.3	0.25	103.407	1.260	5360	4.588	0.860
733.01	10271806	15.6	0.24	102.725	5.925	5038	4.846	0.730
734.01	10272442	15.3	0.39	120.924	24.542	5719	4.700	1.329
736.01	10340423	16.0	0.25	110.789	18.796	4157	4.552	0.681
737.01	10345478	15.7	0.43	115.678	14.499	5117	4.602	0.798
740.01	10395381	15.6	0.17	119.368	17.672	4711	4.640	0.703
743.01	10464078	15.5	1.65	105.491	19.402	4877	4.304	1.904
746.01	10526549	15.3	0.24	106.246	9.274	4681	4.551	0.788
747.01	10583066	15.8	0.28	104.602	6.029	4357	4.680	0.608
749.01	10601284	15.4	0.23	104.806	5.350	5374	4.780	0.915
750.01	10662202	15.4	0.19	104.535	21.679	4619	4.624	0.703
752.01	10797460	15.3	0.26	103.533	9.489	5584	4.406	1.067
753.01	10811496	15.4	2.11	108.840	19.904	5648	4.843	0.621
758.01	10987985	15.4	0.43	109.353	16.016	4869	4.284	1.172

Table A1
(Continued)

KOI	KIC Number	Kp	Planet Radius R_J	Epoch BJD-2454900	Period (days)	T_{eff} (K)	log(g) (cgs)	$R*$ (Sun)
759.01	11018648	15.1	0.32	127.134	32.629	5401	4.563	0.864
760.01	11138155	15.3	0.81	105.257	4.959	5887	4.622	0.830
762.01	11153539	15.4	0.24	104.356	4.498	5779	4.596	1.172
764.01	11304958	15.4	0.71	141.932	41.441	5263	4.367	1.582
765.01	11391957	15.3	0.20	104.629	8.354	5345	4.700	0.722
769.01	11460018	15.4	0.21	104.903	4.281	5461	4.643	0.942
770.01	11463211	15.5	0.26	103.998	1.506	5502	4.927	0.590
772.01	11493732	15.2	0.68	106.831	61.263	5885	4.409	1.079
773.01	11507101	15.2	0.21	105.837	38.374	5667	4.624	0.820
776.01	11812062	15.5	0.55	104.792	3.729	5309	4.829	0.843
777.01	11818800	15.5	2.00	106.564	40.420	5256	4.479	0.948
778.01	11853255	15.1	0.18	103.681	2.243	4082	4.605	0.611
782.01	11960862	15.3	0.59	106.634	6.575	5733	4.411	1.248
783.01	12020329	15.1	0.96	102.991	7.275	5284	4.762	1.953
784.01	12066335	15.4	0.25	119.798	19.266	4112	4.569	0.653
785.01	12070811	15.5	0.21	111.749	12.393	5380	4.725	0.741
786.01	12110942	15.2	0.17	103.366	3.690	5638	4.715	0.876
787.01	12366084	15.4	0.30	104.017	4.431	5615	4.534	1.037
788.01	12404086	15.2	0.31	109.049	26.396	4950	4.634	0.747
789.01	12459725	15.7	0.15	104.505	14.180	5563	4.765	0.683
790.01	12470844	15.3	0.18	107.168	8.472	5176	5.058	0.612
791.01	12644822	15.1	0.79	113.890	12.612	5564	4.528	1.117
793.01	2445129	15.1	0.34	106.313	10.319	5655	4.409	1.069
795.01	3114167	15.6	0.22	103.575	6.770	5455	4.804	0.640
799.01	3246984	15.3	0.41	102.817	1.627	5491	4.412	1.051
802.01	3453214	15.6	0.75	114.881	19.620	5556	5.009	0.498
804.01	3641726	15.4	0.23	110.194	9.030	5136	4.533	0.874
808.01	3838486	15.8	0.37	104.985	2.990	4389	4.582	0.701
810.01	3940418	15.1	0.23	103.507	4.783	4997	4.571	0.820
811.01	4049131	15.4	0.41	114.427	20.507	4764	4.432	0.944
812.01	4139816	16.0	0.22	104.978	3.340	4097	4.661	0.571
813.01	4275191	15.7	0.60	103.528	3.896	5357	4.726	0.725
814.01	4476123	15.6	0.27	108.450	22.368	5236	4.855	0.984
815.01	4544670	15.7	0.90	105.628	34.845	5344	4.485	0.948
819.01	4932348	15.5	1.39	129.933	38.037	5386	4.963	0.518
820.01	4936180	15.3	0.67	106.720	4.641	6287	4.511	0.970
822.01	5077629	15.8	0.95	105.179	7.919	5458	4.605	0.824
823.01	5115978	15.2	0.82	103.228	1.028	5976	4.427	4.223
825.01	5252423	15.3	0.19	109.957	8.103	4735	4.581	0.764
826.01	5272878	15.1	0.21	104.135	6.366	5557	4.843	0.854
827.01	5283542	15.5	0.25	107.779	5.975	5837	4.539	0.918
829.01	5358241	15.4	0.24	107.778	18.649	5858	4.567	0.888
833.01	5376067	15.4	0.39	106.275	3.951	5781	4.660	0.788
834.01	5436502	15.1	0.78	104.372	23.655	5614	4.598	1.496
835.01	5456651	15.2	0.17	113.936	11.763	4817	4.952	0.635
837.01	5531576	15.7	0.16	107.659	7.954	4817	4.751	0.623
838.01	5534814	15.3	0.69	106.011	4.859	5794	4.475	0.991
842.01	5794379	15.4	0.25	108.349	12.719	4497	4.524	0.787
843.01	5881688	15.3	0.56	104.440	4.190	5784	4.396	1.092
845.01	6032497	15.4	0.35	110.290	16.330	5646	4.444	1.224
846.01	6061119	15.5	1.37	119.713	27.807	5612	4.597	0.846
847.01	6191521	15.2	0.70	136.898	80.868	5469	4.559	1.894
849.01	6276477	15.0	0.24	103.936	10.355	5303	4.475	0.956
850.01	6291653	15.3	0.89	109.522	10.526	5236	4.549	0.865
851.01	6392727	15.3	0.50	102.975	4.583	5570	4.551	0.892
852.01	6422070	15.3	0.20	104.904	3.762	5448	4.466	0.980
853.01	6428700	15.4	0.28	102.690	8.204	4842	4.472	0.906
855.01	6522242	15.2	1.21	128.787	41.408	5316	4.586	0.832
856.01	6526710	15.3	0.91	105.855	39.749	5858	4.592	0.861
857.01	6587280	15.1	0.19	107.884	5.715	5033	4.629	0.764
858.01	6599919	15.1	0.86	106.989	13.610	5440	4.450	0.999
863.01	6784235	15.5	0.22	105.152	3.168	5651	4.593	0.851
865.01	6862328	15.1	0.63	155.237	119.021	5560	4.704	1.232
867.01	6863998	15.2	0.32	113.274	16.086	5059	4.521	0.881
868.01	6867155	15.2	1.04	141.431	206.789	4118	4.517	0.927

Table A1
(Continued)

KOI	KIC Number	Kp	Planet Radius R_J	Epoch BJD-2454900	Period (days)	T_{eff} (K)	log(g) (cgs)	$R*$ (Sun)
871.01	7031517	15.2	0.91	112.422	12.941	5650	5.051	0.477
872.01	7109675	15.3	0.65	119.684	33.593	5127	4.592	0.810
873.01	7118364	15.0	0.14	105.226	4.348	5470	4.784	0.789
874.01	7134976	15.0	0.17	102.977	4.602	5037	4.561	0.706
875.01	7135852	15.7	0.34	103.624	4.221	4198	4.865	0.780
876.01	7270230	15.9	0.68	104.898	6.998	5417	4.865	0.589
877.01	7287995	15.0	0.24	103.952	5.955	4211	4.566	0.678
877.02	7287995	15.0	0.21	114.227	12.038	4211	4.566	0.678
878.01	7303253	15.3	0.41	106.808	23.591	4749	4.281	1.160
882.01	7377033	15.5	1.20	103.694	1.957	5081	4.572	0.826
883.01	7380537	15.8	1.05	103.101	2.689	4674	4.821	0.642
887.01	7458762	15.0	0.22	108.345	7.411	5601	4.525	0.923
889.01	757450	15.3	1.52	102.992	8.885	5101	4.480	0.933
890.01	7585481	15.3	0.84	109.623	8.099	5976	4.561	1.104
891.01	7663691	15.1	0.34	109.969	10.006	5851	4.593	1.244
892.01	7678434	15.2	0.23	105.617	10.372	5010	4.604	0.788
895.01	7767559	15.4	1.24	104.894	4.409	5436	4.372	1.195
896.01	7825899	15.3	0.38	108.568	16.240	5206	4.629	0.821
896.02	7825899	15.3	0.28	107.051	6.308	5206	4.629	0.821
900.01	7938496	15.4	0.45	105.339	13.810	5692	4.335	1.172
901.01	8013419	15.8	0.26	109.938	12.733	4213	4.716	0.359
902.01	8018547	15.8	0.83	169.808	83.904	4312	4.616	0.940
903.01	8039892	15.8	0.95	106.433	5.007	5620	4.776	1.256
906.01	8226994	15.5	0.23	107.135	7.157	5017	4.558	0.836
908.01	8255887	15.1	1.11	104.446	4.708	5391	4.245	1.288
910.01	8414716	15.7	0.26	104.720	5.392	5017	4.863	0.876
911.01	8490993	15.4	0.18	104.006	4.094	5820	4.783	0.758
912.01	8505670	15.1	0.22	104.804	10.849	4214	4.608	0.637
914.01	8552202	15.4	0.23	102.731	3.887	5479	4.965	1.126
916.01	8628973	15.1	0.36	104.312	3.315	5401	4.480	0.959
917.01	8655354	15.2	0.29	106.356	6.720	5681	4.478	0.982
918.01	8672910	15.0	0.99	139.583	39.648	5321	4.544	1.038
920.01	8689031	15.1	0.16	123.502	21.802	5330	4.859	0.608
922.01	8826878	15.4	0.24	104.624	5.155	5253	4.456	0.976
923.01	8883593	15.5	0.32	107.901	5.743	5669	4.596	1.024
924.01	8951215	15.2	0.36	106.306	39.478	5951	4.529	0.935
927.01	9097120	15.5	1.46	121.982	23.900	5957	4.557	0.903
931.01	9166862	15.3	1.15	103.679	3.856	5714	4.776	1.011
934.01	9334289	15.8	0.32	106.008	5.827	5733	4.655	0.861
935.01	9347899	15.2	0.40	113.013	20.859	6345	4.696	1.018
937.01	9406990	15.4	0.20	109.572	20.835	5349	4.685	0.725
938.01	9415172	15.6	0.24	104.701	9.946	5342	4.582	0.838
940.01	9479273	15.0	0.54	102.571	6.105	5284	4.629	1.337
942.01	9512687	15.4	0.23	107.857	11.515	4997	4.734	0.663
944.01	9595686	15.4	0.37	103.244	3.108	5166	4.495	0.921
945.01	9605514	15.1	0.23	121.860	25.852	6059	4.594	1.072
948.01	9761882	15.6	0.19	106.717	24.582	5298	4.946	0.706
949.01	9766437	15.5	0.27	103.766	12.533	5733	4.703	0.909
951.01	9775938	15.2	0.58	104.546	13.197	4767	4.255	1.205
955.01	9825625	15.1	0.23	108.731	7.039	6121	4.510	1.141
956.01	9875711	15.2	0.50	108.645	8.361	4580	4.334	1.051

Note. To provide accurate estimates of the epoch and period for observers, data taken after Q1 were used when available.

are the orbital period, epoch, and an estimate of the size of the candidate.

REFERENCES

Agol, E., Steffen, J., Sari, R., & Clarkson, W. 2005, MNRAS, 359, 567
Almenara, J. M., et al. 2009, A&A, 506, 337
Batalha, N. M., et al. 2010, ApJ, 713, L103
Borucki, W. J., et al. 2009, Science, 325, 709
Borucki, W. J., et al. 2010, ApJ, 713, L126
Brown, T. M. 2003, ApJ, 593, L125
Brown, T. M., & Latham, D. W. 2008, arXiv:0812.1305
Caldwell, D. A., et al. 2010, ApJ, 713, L92
Dunham, E. W., et al. 2010, ApJ, 713, L136
Gaudi, B. S. 2005, ApJ, 628, L73
Gautier, T. N., III. 2010, arXiv:1001.0352
Gilliland, R. L., et al. 2010, ApJ, 713, L160
Holman, M. J., & Murray, N. W. 2005, Science, 307, 1288
Jenkins, J. M. 2002, ApJ, 575, 493

Jenkins, J. M., et al. 2010a, arXiv:1001.0416
Jenkins, J. M., et al. 2010b, ApJ, 713, L120
Jenkins, J. M., et al. 2010c, ApJ, 713, L87
Jenkins, J. M., et al. 2010d, Proc. SPIE, 7740, 77400D-1
Johnson, J. J., Aller, K. M., Howard, A. W., & Crepp, J. R. 2010, arXiv: 1005.3084.v2
Koch, D. G., et al. 2010a, ApJ, 713, L131
Koch, D. G., et al. 2010b, ApJ, 713, L79
Latham, D. W., et al. 2010, ApJ, 713, L140
Prsa, A., et al. 2010, arXiv:1006.2815
Santos, N. C., & Mayor, M. 2003, in JENAM 2002, The Unsolved Universe: Challenges for the Future, ed. M. Monteiro (Dordrecht: Kluwer), 15
Steffen, J. H., et al. 2010, arXiv:1006.2763
Tenenbaum, P., Bryson, S. T., Chandrasekaran, H., Li, J., Quintana, E., Twicken, J. D., & Jenkins, J. M. 2010, Proc. SPIE, 7740, 0J-01
Torres, G., Konacki, M., Sasselov, D. D., & Jha, S. 2004, ApJ, 614, 979
Torres, G., Winn, J. N., & Holman, M. J. 2008, in IAU Symp. 253, Toward a Homogeneous Set of Transiting Planet Parameters, ed. F. Pont, D. Sasselov, & M. Holman (Cambridge: Cambridge Univ. Press), 482
Winn, J. N. 2007, in ASP Conf. Ser. 366, Exoplanets and the Rossiter–McLaughlin Effect. Transiting Extrasolar Planets Workshop, ed. C. Afonso, D. Weldrake, & Th. Henning (San Francisco, CA: ASP), 170
Wu, H., et al. 2010, Proc. SPIE, 7740, 774019-1